

NATIONAL ADVISORY COMMITTEE FOR AERONAUTICS

WARTIME REPORT

ORIGINALLY ISSUED

July 1945 as
Memorandum Report E5G09

FLIGHT AND TEST-STAND INVESTIGATION OF HIGH-PERFORMANCE FUELS

IN MODIFIED DOUBLE-ROW RADIAL AIR-COOLED ENGINES

I - DETERMINATION OF THE COOLING CHARACTERISTICS

OF THE FLIGHT ENGINE

By Milton Werner, Calvin C. Blackman, and H. Jack White

**Aircraft Engine Research Laboratory
Cleveland, Ohio**

NACA

WASHINGTON

NACA WARTIME REPORTS are reprints of papers originally issued to provide rapid distribution of advance research results to an authorized group requiring them for the war effort. They were previously held under a security status but are now unclassified. Some of these reports were not technically edited. All have been reproduced without change in order to expedite general distribution.

NACA MR No. E5G09

NATIONAL ADVISORY COMMITTEE FOR AERONAUTICS

MEMORANDUM REPORT

for the

Air Technical Service Command, Army Air Forces

FLIGHT AND TEST-STAND INVESTIGATION OF HIGH-PERFORMANCE FUELS

IN MODIFIED DOUBLE-ROW RADIAL AIR-COOLED ENGINES

I - DETERMINATION OF THE COOLING CHARACTERISTICS

OF THE FLIGHT ENGINE

By Milton Werner, Calvin C. Blackman, and H. Jack White

SUMMARY

The cooling characteristics of a modified 14-cylinder double-row radial air-cooled engine installed in a four-engine airplane were determined from cooling data obtained in a single flight at a pressure altitude of 7000 feet. The tests were conducted in such a manner that the effects of charge-air flow, cooling-air pressure drop, and fuel-air ratio on engine cooling could be separately investigated.

From the results of the cooling-correlation data, the cooling-limited performance relations for normal engine operating conditions were calculated and maximum engine temperature were predicted by means of the cooling equations presented herein. The maximum temperatures predicted for cylinder heads, flanges, and barrels satisfy the manufacturer's limitations for all operating conditions except take-off. Temperature-limited performance as a function of fuel-air ratio and cowl-flap setting was predicted for four-engine operation of the airplane at maximum cylinder-head temperatures of 400° and 450° F. From the predicted temperature-limited performance it appears that the rear-spark-plug-gasket temperature limit would be exceeded before that of the flange. The manufacturer's specification for maximum-cruise power, in combination with the carburetor-metering characteristic curve, is in close agreement with the temperature-limited performance for 400° F maximum head temperature and closed cowl flaps.

INTRODUCTION

At the request of the Air Technical Service Command, Army Air Forces, an investigation to evaluate various high-performance fuel components as blending agents for aviation fuels is being conducted on a modified double-row radial air-cooled engine at the Cleveland laboratory of the NACA.

In order to evaluate the practicability of using high-performance fuels for a given engine installation, it is desirable to compare the cooling-limited power with the knock-limited power; a correlation of the cooling characteristics of the engine was consequently made.

Because the properties of all test fuels are sufficiently alike, insofar as characteristics affecting engine cooling are concerned, the cooling tests were made using the reference fuel (28-R).

The first phase of the flight program consisted in an investigation of the cooling characteristics of the original test engine installed in a four-engine airplane. (See reference 1.) The second phase of the flight program was made with a modified engine because the design changes improved cooling and increased power ratings; the changes are detailed in the appendix. This report, which is the first investigation in the second phase, presents the cooling characteristics of the modified test engine. The correlation of these engine cooling data is based on the method developed in reference 2.

EQUIPMENT AND INSTRUMENTATION

Test engine. - The flight tests were conducted on an R-1830-94 engine mounted in the left inboard nacelle of a B-24D airplane. The engine is a 14-cylinder double-row radial air-cooled engine with a normal rated power of 1100 brake horsepower at 2600 rpm and a take-off power of 1350 brake horsepower at 2800 rpm.

Instrumentation. - A detailed description of the equipment, the instrumentation, the stations at which data were recorded, the differences between the modified (R-1830-94) engine and the original test (R-1830-90C) engine, and the method of setting conditions during tests are given in the appendix. The airplane was so equipped that all data could be recorded within approximately 10 seconds after the 2-minute stabilization period.

The cooling-air pressure drop across the engine was measured by total-pressure tubes in front of the engine and static-pressure tubes at the rear of the engine.

The cooling analysis for the cylinder heads was based on the temperatures of the rear-spark-plug bosses designated T_{38} . These temperatures were measured by 14 embedded thermocouples inserted 30 percent of the head-metal thickness into the rear-spark-plug bosses of the cylinders. The thermocouple junction was located at the bottom of a brass bushing (1/8-in. diam.). The cooling analysis for the cylinder barrels was based on the rear middle-barrel temperatures designated T_6 . The barrel temperatures were measured by thermocouples in the rear middle of the cylinder outer wall between fins 8 and 9, counting from the top fin; this thermocouple junction was peened into a hole 1/16 inch deep in the aluminum of the cylinder muff. The rear-spark-plug-gasket thermocouple T_{12} and the cylinder rear-hold-down-flange thermocouple T_{14} were used to determine temperature limits in accordance with the manufacturer's specifications.

TEST PROCEDURE

A single cooling flight was made with the modified engine installed in a four-engine airplane. The test conditions were as follows: pressure altitude, 7000 feet; low blower ratio; engine speed, 2250 rpm; spark advance, 25° B.T.C. The fuel used was 28-R.

The flight test was divided into three parts:

1. Variable charge-air flow: The charge-air flow was varied while the engine cooling-air pressure drop was maintained approximately constant and the fuel-air ratio was held as close to 0.08 as possible.
2. Variable cooling-air pressure drop: The cooling-air pressure drop was varied while the charge-air flow was maintained approximately constant and the fuel-air ratio was held as close to 0.08 as possible.
3. Variable fuel-air ratio: The fuel-air ratio was varied while the charge-air flow and the cooling-air pressure drop were maintained approximately constant.

Knock data were recorded from a number of flights using 28-R, triptane blend, and xylidine blend fuels at the following engine conditions: engine speed, 1800 to 2250 rpm; high and low blower; spark advance, 25° B.T.C.; carburetor-air temperature, 80° and 100° F. The knock data were used in combination with the variable fuel-air-ratio data of the cooling flight in determining the variation of mean effective gas temperature T_{g_0} with fuel-air ratio.

CORRELATION PROCEDURE

The correlation equation developed in reference 1 is often written

$$\frac{T_h - T_a}{T_{g_h} - T_h} \text{ or } \frac{T_b - T_a}{T_{g_b} - T_b} = K \frac{W_c^n}{(\sigma \Delta p)^m}$$

or

$$\frac{T_h - T_a}{T_{g_h} - T_h} \text{ or } \frac{T_b - T_a}{T_{g_b} - T_b} = K \left(\frac{W_c^{n/m}}{\sigma \Delta p} \right)^m$$

where

T_h	average cylinder-head temperature, °F
T_b	average cylinder-barrel temperature, °F
T_a	cooling-air temperature (computed stagnation temperature at front of engine), °F
T_{g_h}	mean effective gas temperature for heads, °F
T_{g_b}	mean effective gas temperature for barrels, °F
W_c	charge-air flow, pounds per hour/1000
Δp	cooling-air pressure drop, inches of water

σ ratio of cooling-air stagnation density at front of engine to NACA standard density at sea level (stagnation density calculated from free-air pressure and temperature at flight velocity for each test run)

n, m, K constants derived from cooling data

The mean effective gas temperatures were computed from the following equations developed in reference 3:

$$T_{g_h} = T_{g_{h0}} + \Delta T_{g_0} = T_{g_{h0}} + 0.8 \left[T_c + 20.7 \left(\frac{\text{engine rpm}}{1000} \right)^2 \right] \text{ (Heads)}$$

$$T_{g_b} = T_{g_{b0}} + \Delta T_{g_0} = T_{g_{b0}} + 0.42 \left[T_c + 20.7 \left(\frac{\text{engine rpm}}{1000} \right)^2 \right] \text{ (Barrels)}$$

where

ΔT_{g_0} change in mean effective gas temperature, °F

T_c carburetor inlet-air temperature, °F

The values of T_{g_0} , in accordance with previous cooling-correlation practice, were taken as 1086° F for the heads and 536° F for the barrels at a fuel-air ratio of 0.08 and a reference manifold-air temperature of 0° F. Inasmuch as it was found impossible to maintain a constant fuel-air ratio at exactly 0.08, corrections were necessary, when determining the constants m and n , by assuming a portion of a T_{g_0} curve. The calculations for correcting the variations in fuel-air ratio were based on a portion of the T_{g_0} curve obtained with the original test engine previously installed in the four-engine airplane.

The data from the variable charge-air flow runs provide a plot of $T_h - T_a/T_{g_h} - T_h$ and $T_b - T_a/T_{g_b} - T_b$ for the heads and the barrels, respectively, against W_c (fig. 1). The exponent n is the slope of the resulting line. In a similar manner the data from the variable cooling-air pressure-drop runs provide a plot of

$T_h - T_a/T_{g_h} - T_h$ and $T_b - T_a/T_{g_b} - T_b$ against $\sigma\Delta p$ from which the exponent m is obtained. (See fig. 2.) By the use of both the variable W_c and the variable $\sigma\Delta p$ data, a final correlation curve for the heads and the barrels is obtained by plotting $T_h - T_a/T_{g_h} - T_h$ and $T_b - T_a/T_{g_b} - T_b$ against $W_c^{n/m}/\sigma\Delta p$ in figure 3. From these final correlation curves, the constant K is determined. The correlation curves are then used in computing T_{g_0} values for the variable fuel-air-ratio cooling data and all the knock data obtained with the modified test engine in the four-engine airplane.

Because of the difficulty in maintaining constant conditions in flight, corrections had to be made for variations of W_c and $\sigma\Delta p$ when they were supposedly held constant. It was therefore necessary to make a series of preliminary graphs similar to figures 1, 2, and 3 until the error due to the variations in W_c and $\sigma\Delta p$ were reduced, by successive corrections, to a negligible amount.

RESULTS AND DISCUSSION

The cooling equations obtained from the correlation curves for the heads and the barrels (figs. 1, 2, and 3) are as follows:

$$\frac{T_h - T_a}{T_{g_h} - T_h} = 0.270 \frac{W_c^{0.683}}{(\sigma\Delta p)^{0.320}} \text{ or } 0.270 \left(\frac{W_c^{2.134}}{\sigma\Delta p} \right)^{0.320} \quad (\text{Heads})$$

$$\frac{T_b - T_a}{T_{g_b} - T_b} = 0.505 \frac{W_c^{0.742}}{(\sigma\Delta p)^{0.567}} \text{ or } 0.505 \left(\frac{W_c^{1.309}}{\sigma\Delta p} \right)^{0.567} \quad (\text{Barrels})$$

The data from a large number of knock tests made over a wide range of conditions were correlated by the cooling equations and are presented in figure 4 as a plot of T_{g_0} against fuel-air ratio. The T_{g_0} curve for the heads was faired as nearly as possible through the average of the test data while intersecting the initially assumed

temperature of 1086°F at a fuel-air ratio of 0.08. The T_{80} curve for the barrels was faired to intersect the initially assumed temperature of 536°F at a fuel-air ratio of 0.08. The greater number of the test points lie above the barrel T_{80} curve (fig. 4) in the range of fuel-air ratios from 0.06 to 0.09, indicating a discrepancy in the test data for which no explanation is apparent.

The deviations of maximum cylinder temperatures from the average temperatures are shown in figures 5 and 6 for the rear-spark-plug boss and the rear-spark-plug gasket, respectively, and in figures 7 and 8 for the rear middle barrel and the cylinder rear-hold-down flange, respectively. The maximum temperatures specified by the manufacturer (reference 4) are based on the rear-spark-plug-gasket temperatures T_{12} for the heads and upon the cylinder rear-hold-down-flange temperatures T_{14} for the barrels. The cooling correction was based on the average rear-spark-plug-boss temperatures T_{38} for the heads and the average rear middle-barrel temperatures T_6 for the barrels.

In order to compare the temperatures predicted by the cooling equation with those specified by the engine manufacturer, it was necessary to plot average T_{12} against average T_{38} for the heads (fig. 9) and average T_{14} against average T_6 for the barrels (fig. 10). The three curves in figure 10, for different values of cooling-air pressure drop, show that the difference between flange temperatures and middle-barrel temperatures is less for lower cooling air pressure drop. The calculations for predicting maximum flange temperatures were based on rear middle-barrel temperatures, which were converted to flange temperatures by the use of figure 10 at the proper cooling-air Δp . Figure 10, in combination with the Δp for the operating conditions desired, is also used when the manufacturer's specified flange temperature limit of 335°F is converted to the corresponding rear middle-barrel temperatures.

Maximum temperatures predicted for normal operating conditions of the four-engine airplane are tabulated in the last three columns of table I. The operating conditions at an altitude of 7000 feet are based on a carburetor-air temperature of 60°F . Cowl-flap settings and approximate values of Δp for various flight conditions were obtained with the aid of reference 5 and performance

data of the modified test engine in flight. Cowl-flap settings were given as one-third open and closed. The values of $\Delta p/q_c$ (where q_c is impact pressure) for the cylinder heads at cowl-flap settings of one-third open and closed were found in these tests to be 0.70 and 0.61, respectively; the values for the cylinder barrels were 0.59 and 0.51, respectively. These values in combination with q_c at different values of indicated airspeed were then used in determining the approximate values of Δp for various flight conditions. Maximum head, rear-hold-down-flange, and rear middle-barrel temperatures predicted by the cooling equation are within the maximum temperature limitations set by the manufacturer for all conditions except take-off.

During the cooling test, the hottest cylinder head was cylinder 1 for rich mixtures and cylinder 11 for lean mixtures; the hottest cylinder barrel was cylinder 8 for both rich and lean mixtures. Cylinder 6 had the hottest cylinder rear-hold-down flange for the rich mixtures; for the lean mixtures, cylinders 6, 8, and 9 were the hottest.

The predicted temperature-limited brake horsepower and manifold pressure for 1800 and 2250 rpm are shown in figures 11 and 12, respectively. These curves show the horsepower and the manifold pressures expected on each of the four modified test engines during flight of four-engine airplane at a gross weight of 50,000 pounds, an altitude of 7000 feet, a free-air and carburetor-air temperature representative for the knock data, and maximum rear-spark-plug-gasket temperatures of 400° and 450° F. Calculations were made for both one-third open and closed cowl flaps at each of these temperatures. The predicted maximum temperatures of the rear middle barrel and the cylinder hold-down flange corresponding to the temperature-limited curves in figures 11 and 12 are shown in figure 13 for engine speeds of both 1800 and 2250 rpm. From figure 13 it may be seen that the flange temperatures do not exceed the limit (335° F) set by the manufacturer, indicating that the temperature limit for the rear-spark-plug gasket would be exceeded before that of the flange. These estimated temperature-limited relations were determined by the use of the cruise control chart (reference 5) for the airplane and the air-flow manifold-pressure data obtained from flight-knock tests with 28-R, triptane blend, and xylidine blend fuels. An enumeration of the assumptions made in these calculations may be found in reference 6, which presents similar data for the original test engine. The engine manufacturer's instructions for maximum cruise with the modified test engine specify a manifold pressure of 31.2 inches of mercury absolute at 2250 rpm, low blower ratio, cowl flaps closed, and automatic lean-mixture setting.

The curve for automatic-lean carburetor-metering characteristics in figure 12 indicates that this cruising power falls close to the predicted temperature-limited performance curve for a maximum rear-spark-plug-gasket temperature of 400° F with cowl flaps closed.

SUMMARY OF RESULTS

The following cooling characteristics apply to the modified 14-cylinder double-row air-cooled engine installed in a four-engine airplane:

1. The cooling equation for the modified test engine was:

$$\frac{T_h - T_a}{T_{g_h} - T_h} = 0.270 \frac{W_c^{0.683}}{\sigma \Delta p^{0.320}} \quad (\text{Heads})$$

$$\frac{T_b - T_a}{T_{g_b} - T_b} = 0.505 \frac{W_c^{0.742}}{\sigma \Delta p^{0.567}} \quad (\text{Barrels})$$

2. Temperature-limited performance as a function of fuel-air ratio and cowl-flap setting was predicted for four-engine operation of the airplane at maximum head temperatures of 400° and 450° F. From the predicted temperature-limited performance, it appears that the temperature limit set by the manufacturer for the rear-spark-plug gasket would be exceeded before that of the flange. The manufacturer's specifications for maximum cruise at 2250 rpm agree with the temperature-limited power for a maximum rear-spark-plug-gasket temperature of 400° F with cowl flaps closed.

3. From the results of the cooling-correlation data, maximum engine temperatures were predicted for normal flight conditions of the airplane. Maximum head, rear-hold-down-flange, and rear middle-barrel temperatures predicted by the cooling equation are within the maximum temperature limitations set by the manufacturer for all conditions investigated except take-off.

Aircraft Engine Research Laboratory,
National Advisory Committee for Aeronautics,
Cleveland, Ohio, July 9, 1945.

APPENDIX - EQUIPMENT, INSTRUMENTATION, AND FLIGHT-TEST PROCEDURE

By Milton Werner and S. Joseph Lamancusa

This appendix has been prepared to set forth in detail the equipment, the instrumentation, and the fuel flight-test procedure used in the tests of the R-1830-90C (original) and R-1830-94 (modified) engines. The description contained herein will be used as reference material for several reports to follow.

The knock data required in tests of each engine in flight were recorded while the engine was operated at knock-limited power. In order to reduce the time of operation at knock-limited power, the engine and the airplane were instrumented to record all test data within a very short time after stabilization of conditions. The time required for data to be recorded was, in general, only slightly over 10 seconds owing to the use of special film-recording instruments of high sensitivity and speed. Considerable duplication of measurements was obtained because of the use of both indicating and recording instruments.

In order to facilitate setting engine conditions and to minimize the likelihood of engine failure, many of the primary engine variables (engine speed, manifold pressure, carburetor-air temperature, blower ratio, fuel flow, and torque) were indicated at several stations on gages. These engine variables were also recorded on film. Most of the gages on which the engine variables were indicated for visual inspection were also photographed. Cylinder-head temperatures were indicated on gages and recorded by galvanometers. Engine cooling-air pressures were indicated on a 100-tube manometer and most of these pressures were recorded by a 60-cell manometer. The duplication of records provided a check and an additional source for most of the data so that a flight need not be repeated even though certain instruments may not have been operating properly. The data of primary interest required consisted essentially of the intensity and the distribution of knock, pressure and temperature measurements, and the measurement of variables necessary for the determination of engine power and airplane performance.

Features of Test Equipment

Design changes. - The manufacturer's design features incorporated in the modified test engine (reference 4) that differed from the original test engine are as follows:

1. The cooling area on the cylinder heads and barrels has been increased. A greater number of fins is used around the intake and exhaust ports and the integral steel fins on the barrels (on original engine) have been replaced by an aluminum muff with increased fin depth.

2. The increased mechanical strength of engine parts and the improved cooling resulted in increased power ratings.

3. The supercharger-impeller diameter has been increased from 11 to 11.3 inches.

4. An injection carburetor PD-12F7 has replaced the PD-12F2-16 carburetor.

5. Fuel is injected at the impeller by a fuel-discharge spinner nozzle at the impeller entrance rather than by the carburetor with a crab-bar.

6. SF-14LN-8 magnetos are mounted on the nose section in front of cylinders 1 and 13.

7. The cams have been redesigned to include a dual-cam drive.

8. A revision of the valve timing (16° increase in valve overlap) allows higher engine speeds.

9. An automatic two-position spark advance, 25° and 32° B.T.C., has been installed to provide low-power cruising operation of the engine at higher spark advance.

Test changes. - The changes made for testing the modified engine are as follows:

1. The fuel-transfer line from the carburetor to the fuel-injection valve required alteration to adapt the original (crab-bar injection) carburetor to the modified engine, which is designed for spinner-impeller injection. This change permitted the standard spinner-impeller injection system to be used with the test carburetor.

2. The automatic control for spark setting was replaced by a manual control.

Engine Instrumentation

The airplane, and the installation of knock-detection apparatus, pressure-measuring tubes, and thermocouples are best described by means of figures 14 to 21. The location and method of mounting the knock pickups, the pressure tubes, and the thermocouples may be easily seen in these figures.

Knock-detection equipment. - A schematic diagram of the knock-detection equipment is shown in figure 15. A pressure-sensitive pickup of the magnetostriction type was inserted into the combustion chamber of each cylinder. The pickups convert changes in combustion pressures and vibrations within the cylinders to electrical impulses. These impulses, amplified to energize the vertical deflecting plates of the oscilloscope, are manifested by vertical movements of the electron beam on the fluorescent screen. The 24-volt direct-current output from a storage battery was changed to 110 volts alternating current in the inverter. The output from the inverter in combination with an engine-driven timer provided the electromotive force to the horizontal deflecting plates and produced the horizontal sweep of the electron beam across the screen in direct synchronization with the engine. A diagram showing rate-of-pressure change against time was obtained with this installation.

Three oscilloscopes were used to permit the diagrams of three cylinders to be viewed at one time. A complete survey of all cylinders could be made within a few seconds by means of a special selector switch. This switch also operated the sequence cylinder lights, which identified the cylinders appearing on the oscilloscopes at a given time. In order that the combustion portion of the diagrams for all cylinders would appear at the center of their respective oscilloscope screen, it was found convenient to provide the equivalent of five independent engine-driven contactors. This feature was achieved by means of a long camshaft provided with five "flats," all at different angles with respect to a given crankshaft position. Each flat operated a separate breaker-point assembly, as shown in figure 15. Detection of preignition was facilitated by this provision because any deviation of the diagram from the center of the screen indicated an irregularity in the combustion process.

Thermocouples. - All thermocouples were 24-gage iron-constantan junctions except those in the exhaust stack and the oxidizing furnace, which were 22-gage chromel-alumel junctions. Three thermocouples were located on the head and two on the barrel of each cylinder. A bare thermocouple for measuring mixture temperature was inserted into the center of each intake manifold. A thermocouple for measuring carburetor-air temperature was mounted on the carburetor screen.

The head temperatures were measured by an embedded thermocouple in the front-spark-plug boss T_{36} , an embedded thermocouple in the rear-spark-plug boss T_{38} , and by a thermocouple on the rear-spark-plug gasket T_{12} . Details of the installation of a typical embedded rear-spark-plug-boss thermocouple are shown in figure 16. Both embedded thermocouples T_{36} and T_{38} were inserted 30° toward the exhaust side; T_{12} was of the conventional flange type with a double junction, one for indicating the temperature on individual gages and the other for recording the temperature on a galvanometer. The barrel temperatures were measured by a thermocouple T_6 , which was peened $1/16$ inch into the rear middle of the aluminum muff between fins 8 and 9, counting from the top. Additional measurements were taken from thermocouples inserted through the aluminum muff to contact the steel of the barrel. This thermocouple provided a temperature check between the thermocouple peened into the aluminum muff and the thermocouple contacting the steel of the barrel. Negligible difference in temperature was observed, however, between these two thermocouples. Flange temperatures were indicated by a cylinder rear-hold-down-flange thermocouple T_{14} . The junction of T_{14} was spot-welded to the fillet of the steel flange at the rear of the cylinder, which location corresponds to that specified by the manufacturer for the limiting-barrel temperatures. (A spot-welded thermocouple is not recommended for similar tests because an engine failure resulted from a fatigue crack that originated at one of these spot welds.) The location and method of mounting thermocouples T_{36} , T_{38} , T_{12} , T_6 , and T_{14} are shown in figures 17 to 20. The mixture temperature for each cylinder was measured by locating a bare thermocouple at the center of each intake manifold at a distance of approximately $8\frac{1}{2}$ inches from the outer case of the supercharger. The thermocouple for measuring carburetor-air temperature was mounted on the carburetor screen with the iron junction over one venturi and the constantan junction over the other venturi of the carburetor with a common wire of the screen joining the two junctions. Free-air temperature was measured by means of a six-junction thermopile.

Fuel-flow measurements. - Measurements of fuel flow were made by three independent methods: a deflecting-vane-type fuel flowmeter, an electrical-type indicating fuel flowmeter (reference 7) that measures a temperature difference created in the fluid by the addition of electrically generated heat (called an NACA thermal flowmeter

hereinafter), and a fuel rotameter. The fuel flow as indicated by the deflecting-vane-type flowmeter was used for most computations; however, the readings of the thermal flowmeter and the rotameter, in general, checked those of the deflecting-vane-type flowmeter very closely.

The deflecting-vane-type fuel flowmeter was installed in the fuel-transfer line between the carburetor and the fuel-injection valve. This provision eliminated the chance for errors in fuel-flow measurement as a result of backflow of liquid fuel through the carburetor vapor eliminator. In addition, a solenoid shut-off valve in the vapor-eliminator line permitted the flow in this line to be stopped for the brief interval in the test sequence when rotameter readings were being taken. The rotameter was located in the line between the fuel tanks and the engine fuel pump and was mounted in the bomb bay. In certain instances (usually at low values of fuel flow) the rotameter was found to give erratic readings, which were attributed to sticking of the bob on the guide rod. Inasmuch as readings from the rotameter checked the deflecting-vane-type meter over the rest of the range, the deflecting-vane-type data were generally used.

Exhaust-gas-sampling system. - Exhaust gas was drawn into the sampling system through a 1/4-inch impact tube located in the main exhaust stack immediately downstream of the engine collector-ring outlet. This gas was then passed through heated, oxidizing elements filled with copper oxide in wire form, which converted all the carbonaceous products of normal combustion other than CO_2 (CO , CH_4 , free carbon, and others) into CO_2 and water vapor. The oxidizing unit was mounted in an enlarged section of the main exhaust stack as shown in figure 21 so that the greater portion of the heat necessary for this reaction would be supplied by the hot exhaust gases passing to the turbosupercharger. Electric heating coils provided additional heating of the elements in such cases when sufficient heat was not available from the exhaust gases. After being passed through a CaCl_2 desiccator (drying) unit, the exhaust-gas sample was conducted to the rear of the airplane where three separate analyses were made by Orsat apparatus for each test point to determine the CO_2 content of the oxidized samples. Fair agreement was obtained between fuel-air ratios by means of the average of the three Orsat analyses and by calculations from measured fuel flow and air flow.

Carburetor. - A PD-12F2-16 carburetor was used because complete air-flow calibration data were available for it (from tests of references 1 and 6) and because it permitted fuel-air ratio to be varied over a somewhat wider range than would be available from the standard PD-12F7 carburetor for the modified engine. Sensitive control of fuel flow in the lean-mixture range was simplified by the use of the specially contoured (cruising) mixture-control plate supplied by the carburetor manufacturer.

Charge-air-flow measurements. - The carburetor was given the standard air-flow calibration in an air box with part of the upstream ducting from the airplane in place. It was found necessary to check this calibration with the carburetor in the airplane with turbosupercharger, intercooler, and all ducting in operation. A special duct, which was equipped with a sharp-edged entrance orifice and a two-dimensional pressure-tube rake, was installed ahead of the turbosupercharger for an accurate determination of charge-air flow during a ground test. As a result of this investigation, a correction curve was established, which was used in conjunction with the standard air-box calibration when determining rate of air flow in flight from measurements of carburetor-metering pressures, total pressure at the carburetor face, and carburetor-air temperature. A typical chart is included (fig. 22) that shows an approximate method by which charge-air flow and fuel-air ratio were rapidly determined during flight. Curves similar to those on the upper portion of figure 22, but based on uncompensated metering pressures, were used for accurate computation of air flow in the final reduction of the data.

Cooling-air pressure tubes. - The cooling-air pressure tubes were of 1/8-inch copper with a 0.090-inch stainless-steel tip at the entrance. The cooling-air pressure tubes used in the cooling correlation are underlined in figure 23. The tubes for determining the pressure drop across the engine consisted of the total-pressure tubes at the baffle entrance to the front-row cylinders (figs. 17 and 23) and static-pressure tubes in the baffle-exit curl and behind the top head baffle of the rear-row cylinders. (See figs. 18, 20, and 23.) Static tubes were located as nearly as possible at the same height (measuring radially from the cylinder-base flange) as the total-pressure tubes. Pressure tubes were mounted at the baffle entrance to the rear-row cylinders at the same relative location on the cylinders as the front-row cylinders; however, a different method of mounting the tubes was necessary for this particular baffle arrangement. (See fig. 19)

Miscellaneous. - Manifold pressures were indicated by a sensitive manifold-pressure gage. A hydraulic torquemeter was used in determining engine power. A modification of the torque-nose oil boost capacity was unnecessary for the modified test-engine torquemeter, whereas additional boost capacity was necessary for the measurement of high engine powers with the original test-engine torquemeter. (See reference 6.) Engine and turbosupercharger rotational speeds were indicated by tachometers.

Computation of Average Cooling-Air Pressure Drop

The cooling-air pressure drop across the engine for the cylinder heads was taken as the differential pressure between the total pressure in front of the engine and the static pressure at the rear of the engine. The total pressure was taken as the average of three total-pressure tubes at the baffle entrance of each of the front-row cylinder heads and the static pressure as the average of the static pressures in the stagnation region behind the head baffle and in the baffle-exit curl of each of the rear-row cylinder heads. For the cylinder barrels the engine cooling-air pressure drop was taken in a similar manner but with only two total pressures at the baffle entrance and one static pressure in the baffle exit curl. Figure 23 is a schematic diagram of a front-row and a rear-row cylinder as seen from the front of the engine and shows relative positions of all total- and static-pressure tubes as mounted on the cylinders and their location with respect to the engine zones used for computing average cooling-air pressure drops.

Average cylinder-head pressure drop for the engine was computed as follows: The total pressure for a particular tube location was averaged for the seven front-row cylinders; for example

$$\text{av. } H_{ah11} = \frac{1}{7} \left(H_{ah11} \text{ for cylinders 2, 4, 6, 8, 10, 12, and 14} \right)$$

in similar manner, for static pressures

$$\text{av. } p_{ah2} = \frac{1}{7} \left(p_{ah2} \text{ for cylinders 1, 3, 5, 7, 9, 11, and 13} \right)$$

This process was repeated for each of the three total-pressure-tube locations on the front-row cylinders and for each of the two static-pressure-tube locations on the rear-row cylinders. Average engine pressure drop for heads was then computed by use of the aforementioned averages as follows:

$$\text{av. } \Delta p = \frac{1}{3} \left(\text{av. } H_{ah11} + \text{av. } H_{ah12} + \text{av. } H_{ah13} \right) - \frac{1}{2} \left(\text{av. } P_{ah2} + \text{av. } P_{ah3} \right) \quad (\text{Heads})$$

The analysis for average barrel pressure drop for the engine followed the same pattern as given for the heads. In this case the following measurements were involved:

$$\text{av. } \Delta p = \frac{1}{2} \left(\text{av. } H_{ab11} + \text{av. } H_{ab12} \right) - \text{av. } P_{ab2} \quad (\text{Barrels})$$

General Airplane Instrument Installation

The general installation of instruments and their location according to stations in the airplane are shown in figure 24. A tabulation of the instruments and the data recorded at each station is given in table II.

Station 1. - Figure 25 shows the auxiliary instrument panel, the carburetor-air-temperature indicator, and the signal system for communication with other stations in the airplane. The instruments used by the pilot at station 1 for setting engine conditions were observed during the tests, but their readings were not recorded inasmuch as these measurements are indicated and recorded elsewhere. A complete list of instruments at station 1 is given in table II, column 1.

Station 2. - The flight coordinator operated the equipment at station 2 (fig. 26), which consisted of the main test instrument panel, the main signal system for communications with other stations, and all controls for operating special film-recording instruments. The instruments at station 2 were photographed during flight and are listed in table II, column 2. In column 3 is a list of measurements taken with the special film-recording instruments.

Station 3. - At station 3 (fig. 27) the existence of knock on any of the 14 cylinders could be observed by the use of three oscilloscopes in combination with a selector switch. The sequence signal lights identified the group of cylinders that was being viewed on the oscilloscopes.

Station 4. - Fuel selection was made by the flight mechanic at station 4 in the rear bomb bay compartment (fig. 28). Readings taken by the flight mechanic are shown in column 5 of table II.

Station 5. - The observer at station 5 (fig. 29) operated the NACA thermal fuel flowmeter, recorded special temperatures and reference voltage for the recording instruments, and checked the operation of the recording instruments.

Station 6. - At station 6 were three Orsat apparatuses and an NACA fuel-air ratio indicator (fig. 30). Three individual samples of oxidized exhaust gas were analysed for each test point and their average volumetric CO₂ content was used in determining the fuel-air ratio from a conversion chart.

Station 7. - At station 7 (fig. 31) photographs were taken of the engine cooling-air pressures indicated on the 100-tube manometer board. A continuous record of the rear middle-barrel temperatures was made on a recording flight potentiometer. Continuous visual observation of these readings was desired because those were believed to be the most critical engine temperatures. This judgment was based on the sequence of events, which occurred when a piston failure was experienced during tests with the original test engine. (See reference 6.) An incipient piston seizure can be anticipated by a close scrutiny of these temperatures.

Miscellaneous. - Impact pressure was measured with an NACA total-head tube and static pressures with an NACA swiveling static-pressure tube. Both the total-head and the static-pressure tubes were mounted on a boom extending ahead of the left wing. Figure 32 shows a view of the entire interior of the rear compartment of the airplane. Recording instruments were mounted on the deck ahead of stations 5 and 6 and consisted of pressure, temperature, and rotative-speed (engine and turbosupercharger speed) film recorders.

Procedure for Setting Conditions in Flight for Knock Tests

Stations 1, 2, and 3 were most important in determining conditions of knock and in maintaining constant conditions during a test run. The pilot obtained knock either by leaning the mixture or by increasing the manifold pressure and was notified of the presence of knock by the oscilloscope operator at station 3. Assuming that a knock point had just been obtained (point a, fig. 33) and all the data had been taken, the pilot then reduced the throttle opening to a point below knock, represented by point b. The mixture-control plate was meanwhile held in a constant position. During this reduction of boost (from a to b) the mixture strength would be expected to lean out, corresponding to the shape of the carburetor-metering-characteristic curve in this region. Then, at constant throttle

position (and, consequently, constant manifold pressure) the mixture was leaned out to some point represented by c. After the pilot had reduced the mixture strength by a suitable amount, he gradually increased the manifold pressure, holding constant the mixture control-plate setting, until the oscilloscope operator notified him that proper knock conditions had been reached for another knock point, represented by point d in figure 33.

The carburetor-air temperature was set by the pilot by either of two methods: by adjusting the intercooler-flap opening or by a combination of waste-gate and throttle setting. Measurements from a resistance bulb, which was mounted in the carburetor elbow directly above the carburetor face, were indicated on the pilot's carburetor-air temperature gage. This location corresponds to that of the standard installation in an airplane. It was more convenient to set the carburetor-air temperature from the bulb than from the thermocouple mounted on the carburetor screen because the bulb allowed direct temperature indication, viewed by the pilot, whereas the thermocouple temperatures were recorded on film and indicated only on a manually balanced potentiometer at station 2.

The operator at station 2 was engaged in determining fuel-air ratio (from a chart similar to fig. 22) and plotting the knock data for the previous knock run while the operators at stations 1 and 3 were setting conditions for a new run. When conditions had stabilized, the operator at station 2 photographed the instrument panel and notified the other stations that data should be taken. The other observers were notified by signal lights, which were energized at the moment a switch for the recording instruments was thrown.

Presentation of Data

Measurements from all stations, including flight recorders, and results from a considerable amount of calculations on the data are tabulated on a single data sheet as shown in table III; these data are not from the tests of this paper but are included to show the method of tabulation. This sheet was set up for convenience and ease of handling test measurements; such a sheet contains data for only a single test point.

REFERENCES

1. Blackman, Calvin C., White, H. Jack, and Pragliola, Philip C.: Flight and Test-Stand Investigation of High-Performance Fuels in Double-Row Radial Air-Cooled Engines. I - Determination of the Cooling Characteristics of the Flight Engine. NACA MR No. E4L20, 1944.
2. Pinkel, Benjamin: Heat-Transfer Processes in Air-Cooled Engine Cylinders. NACA Rep. No. 612, 1938.
3. Corson, Blake W., Jr., and McLellan, Charles H.: Cooling Characteristics of a Pratt & Whitney R-2300 Engine Installed in a NACA Short-Nose High-Inlet Velocity Cowling. NACA ACR No. L4F06, 1944.
4. Anon.: Operating Instructions R-1830-94 Engine. PWA. OI. 48A, Pratt & Whitney Aircraft, Dec. 28, 1944.
5. Anon.: Flight Manual, B-24D and J Heavy Bombardment Airplane. Consolidated Vultee Aircraft Corp., Jan. 1944.
6. White, H. Jack, Blackman, Calvin C., and Werner, Milton: Flight and Test-Stand Investigation of High-Performance Fuels in Double-Row Radial Air-Cooled Engines. II - Flight Knock Data and Comparison of Fuel Knock Limits with Engine Cooling Limits in Flight. NACA MR No. E4L30, 1944.
7. Tozier, Robert E.: An Electrical-Type Indicating Fuel Flowmeter. NACA ACR, Sept. 1939.

TABLE I - COMPARISON OF MANUFACTURER'S TEMPERATURE LIMITS WITH PREDICTED MAXIMUM TEMPERATURES
AT NORMAL OPERATING CONDITIONS FOR MODIFIED TEST ENGINE

Operating condition	Engine speed (rpm)	Manifold pressure (in. Hg abs.)	Brake horsepower (nominal)	Mixture setting	Cowl-flap position	Manufacturer's temperature limits (°F)			Predicted maximum temperatures ^e (°F)		
						Head ^a	Flange ^b	Barrel ^c	Head ^a	Flange ^b	Barrel ^d
Military power	2800	50.8	1350	Automatic rich	1/3 open	500	335	287	456	337	289
Take-off	2800	52.0	1350	Automatic rich	1/4 to 1/3 open	500	335	303	543	405	362
Normal rated power	2600	42.7	1100	Automatic rich	1/4 to 1/3 open	450	335	287	440	334	286
Maximum cruise	2250	31.2	735	Automatic lean	Closed	450	335	312	400	283	271
Cruising maximum bmep	1900	29.0	650	Automatic lean	Closed	450	335	320	413	296	288
Normal landing approach	2550	20.0 (approx.)	-----	Automatic rich	Partly open	-----	-----	-----	516	389	366

^aRear-spark-plug-gasket temperatures T_{12} .

^bCylinder rear-hold-down-flange temperatures T_{14} .

^cEstimated maximum rear middle-barrel temperatures T_6 corresponding to a specified flange temperature of 335° F and estimated cooling-air pressure drops.

^dRear middle-barrel temperatures T_6 .

^eCalculations for take-off power and normal landing approach based on sea level pressure altitude and cooling-air and carburetor-air temperatures of 100° F. Other operating conditions based on pressure altitude of 7000 feet and cooling-air and carburetor-air temperatures of 60° F.

TABLE II
LOCATION OF CONTROL EQUIPMENT OR INSTRUMENTS AND STATIONS WHERE DATA WERE RECORDED OR OBSERVED

	1	2	3	4	5	6	7	8
	Station 1, pilot and copilot	Station 2, flight coordinator Panel gages	Station 3, knock observer Recording instruments at stations 4 and 5	Station 4, flight mechanic	Station 5, observer	Station 6, observer	Station 7, observer	Station 8, observer
Knock								
Oscilloscopes				x				
Knock selector switch and lights				x				
Knocking time				x				
Pressures								
Manifold	x	x	x					
Engine torque	x	x	x					
Exhaust	x	x	x					
Carburetor venturi static		x	x					
Carburetor deck		x	x					
Uncompensated metering		x	x					
Compensated metering	x	x	x					
Charge air after turbosupercharger		x	x					
Supercharger throat		x						
Fuel injection		x						
Free-air static (altitude)	x	x	x					
Free-air total (airspeed)	x	x	x					
Cooling-air reference			x					
Cooling air 14 cylinders: P _{ah} 11								x
P _{ah} 12			x					x
P _{ah} 13			x					x
P _{ah} 11			x					x
P _{ah} 12			x					x
Cooling air, 9 cylinders: P _{ah} 2, P _{ah} 3			x					x
P _{ah} 2			x					x
Approximate cooling air Δp (P _{ah} 12 - P _{ah} 11)	x	x						
Temperatures								
Charge air after turbosupercharger			x					
Oil into oil cooler	x		x					
Oil out of oil cooler			x					
Fuel		x						
Carburetor screen	x	x	x					
Magneto			x					
Accessory compartment			x					
Free air		x	x			x		
Instrument		x				x		
Cold junction						x		
Galvanometer reference						x		
Exhaust						x		
Furnace						x		
Dry bulb					x			
Wet bulb					x			
Mixture, 14 cylinders			x					
Rear-spark-plug gasket T ₁₂ , 14 cylinders		x	x					
Embedded rear-spark-plug boss T ₃₈ , 14 cylinders			x					
Embedded front-spark-plug boss T ₃₆ , 14 cylinders			x					
Rear middle barrel T ₆ , 14 cylinders								x
Rear-hold-down flange T ₄ , 14 cylinders			x					
Miscellaneous								
Engine speed	x	x	x					
Turbosupercharger speed	x	x	x					
Blower ratio	x	x						
Mixture control setting	x	x						
Cowl-flap opening	x	x						
Waste-gate setting	x	x						
Intercooler setting		x						
Throttle setting	x	x						
Inclination of thrust axis								x
Fuel selection					x			
Fuel flow (deflecting-vane type)	x	x				x		
Fuel flow (rotameter)					x			
Fuel flow (NACA thermal)						x		
Fuel-air ratio (Orsat)							x	
Fuel-air ratio (NACA)							x	
Fuel-air ratio (computed)		x						
Station communication signals								
Knock	x	x		x				
Fuel vent (solenoid)	x							
Ready lights, Station 1	x	x						
3		x		x				
4		x			x			
5		x				x		
6		x					x	
7		x						x
All ready	x	x		x	x	x	x	x
Run lights	x	x		x	x	x	x	x

TABLE III.-

TABULATED DATA SHEET

Flight 31
Run 4
Date 9-26-44

100-TUBE MANOMETER PRESSURES ^a									60-CELL RECORDER PRESSURES ^b								
Cyl.	Hah 11	Hah 12	Hab 11	Hab 12	Hah 13	Pah 2	Pab 2	Pah 3	Hah 11	Hah 12	Hab 11	Hah 13	Pah 2	Pab 2	Pah 3		
1	15.8	15.5	15.8	15.6	16.0	-2.7	-3.1	-3.2	---	---	---	---	-1.4	-2.9	-3.2		
2	15.2	17.2	13.1	15.8	16.8	---	---	---	14.5	16.5	13.1	16.2	---	---	---		
3	17.9	16.3	17.0	16.7	17.7	-2.0	-1.6	-2.8	---	---	---	---	-2.0	-1.6	-2.9		
4	19.5	19.0	18.3	18.0	18.7	---	---	---	18.2	18.4	17.8	---	---	---	---		
5	19.7	18.2	18.5	19.3	19.4	-1.4	-.9	-2.4	---	---	---	---	-1.6	-.8	-2.3		
6	20.1	18.3	18.7	19.1	20.2	---	---	---	19.2	17.6	18.2	---	---	---	---		
7	19.2	18.1	18.3	18.2	18.5	-.7	-.4	-3.0	---	---	---	---	---	---	-.5	-2.8	
8	18.8	19.7	17.4	16.8	19.0	---	---	---	18.5	18.7	16.7	---	---	---	---		
9	17.6	16.4	17.1	16.9	16.8	-2.7	-2.0	-2.7	---	---	---	---	-2.6	-2.1	-2.8		
10	18.3	18.1	16.8	16.4	18.3	---	---	---	17.7	18.1	16.8	17.7	---	---	---		
11	18.1	16.7	17.0	16.9	17.1	-1.4	-.3	-2.0	---	---	---	---	-1.5	-.5	-2.2		
12	17.7	17.5	15.5	14.7	16.8	---	---	---	17.1	16.6	16.5	---	---	---	---		
13	17.2	14.9	16.2	16.2	16.0	-1.6	-.8	-2.8	---	---	---	---	---	---	-.8	-2.7	
14	15.9	15.7	15.5	14.0	17.2	---	---	---	15.4	15.2	15.2	15.4	---	---	---		
FR Av.	17.9	17.9	16.5	16.4	18.1	---	---	---	17.2	17.3	16.3	16.4	---	---	---		
RR Av.	17.9	16.6	17.1	17.1	17.4	-1.5	-1.3	-2.7	---	---	---	---	-1.8	-1.3	-2.7		
Eng Av.	17.9	17.3	16.8	16.8	17.8	---	---	---	---	---	---	---	---	---	---		

^aRecorded in inches of water.^bRecorded in inches of water.

TEMPERATURES, °F										CONDITION OF KNOCK	
Cyl.	T ₁ (oil)	T ₁₂ (oil)	T _{12A} (oil)	T ₁₆ (oil)	T ₁₄ (oil)	T ₁₈ (oil)	T ₁₉ (oil)				
1	269	460	445	410	303	475	185			Trace	
2	288	380	420	403	323	450	185				
3	267	360	370	395	285	463	188				
4	281	430	415	393	315	443	188			Occasional light	
5	261	420	410	375	265	453	188			Trace	
6	273	430	410	395	330	443	188			Trace	
7	253	410	410	380	295	445					
8	310	420	430	415	320	455	185			light	
9	273	400	385	368	313	440	185				
10	265	440	433	395	300	445	185			Occasional light	
11	267	420	425	355	303	450	185				
12	269	410	---	390	310	443	185				
13	272	440	395	385	305	435	165				
14	297	440	420	435	295	445				Trace	
FR Av.											
RR Av.											
Eng Av.	275	419	413	392	304	449	184				

NATIONAL ADVISORY
COMMITTEE FOR AERONAUTICS

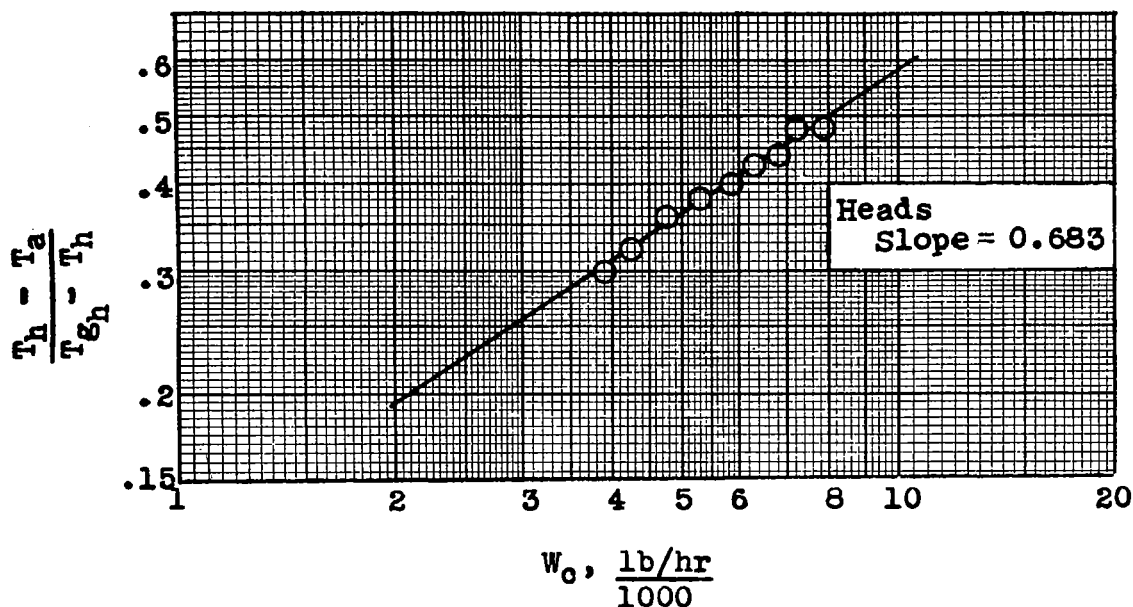
READING	inst panel	60-cell magno	St'nd base
Engine speed, rpm	2250	---	2244
Turbo speed, rpm	15250	---	15276
Indicated airspeed, V _i , mph	206	---	209
Pressure altitude, Z _p , ft	6960	---	7170
Manifold pressure, P _{cc} , in. Hg abs	63.6	---	63.5
Torque, Q, lb-ft	3390	---	3366
Exhaust-back pressure, P _e , in. Hg abs	36.1	---	---
Venturi static pressure, P _{cc} , in. Hg abs	27.7	27.8	---
Carburetor-deck pressure, P _{cd} , in. Hg abs	34.0	33.8	---
Comp. metering pressure, (Hcc1-Pcc), in. H ₂ O	81.0	79.9	---
Uncomp. metering pressure, (Hcc0-Pcc), in. H ₂ O	84.4	82.5	---
Charge air after turbo, P _{ct} , in. Hg abs	---	32.1	---
Engine press. drop, (Hah12-12-Pah3-11), in. H ₂ O	19.4	---	---
Oil pressure into engine, P _{oi} , lb/sq in.	---	---	---
Supercharger throat pressure, P _s , in. Hg abs	32.1	---	---
Fuel-injection pressure, P _i , lb/sq in.	9.0	---	---

Eng	Engine speed (rpm)	Manifold pressure (in. Hg)	Cowl flaps		
1	2250	36	1/4 open		
3	"	"	"		
4	"	"	"		

ADDITIONAL TEMPERATURES		°F
Average mixture, T _{cm}		175
Charge air after turbo, T _{ct}		145
Oil into oilcooler, T _{oi}		203
Oil out of oilcooler, T _{oo}		150
Ind. free-air, T _{fa}	boom	---
	belly	51
	gage	52
	galvanometer	50
True free-air, T _{fa}	---	46.4
	gage	90
	pilot	84
	galvanometer	90
Carburetor screen, T _{cc}		---
Stagnation, T _s		56.1
Left magneto, T _{y-1}		105
Right magneto, T _{y-2}		125
Rear accessory, T _r		83
Instrument, T _i		62
Exhaust gas, T _e		1664
Fuel, T _f	carburetor	71
	rotameter	66
Dry bulb, T _d		57
Wet bulb, T _w		54

True airspeed, V, mph		233
Q _{cc} , in. H ₂ O		21.5
Mach number, M		.310
Fuselage reference press., Δp, in. H ₂ O		1.2
Density altitude, Z _d , ft		8010
Density ratio, ρ/ρ ₀		.7859
Blower ratio		high
Mixture-control setting, deg		36.3
Cowl-flap opening, deg		21.4
Waste-gate setting, deg		32.3
Intercooler-flap opening, percent		87.7
Throttle setting, deg		82.5
Inclination of thrust axis, α, deg		091
Brake horsepower		1138
bmeep, lb/sq in.		277.3
Air flow, lb/hr		9800
Type of fuel		b80-20
Fuel flow, lb/hr	deflecting position #2	a 860
	vane type position #5	870
	rotameter	850
	thermal flowmeter	848
bsfc, lb/hp-hr		.598
F/A	Orsats	.0879
	NACA indicator	.080
	carburetor	.0878
Head pressure drop, in. H ₂ O		20.1
Barrel pressure drop, in. H ₂ O		17.8
Spark setting, deg		25

^aValues used.^b80-20: 80% 28-R, 20% triptane.



NATIONAL ADVISORY
COMMITTEE FOR AERONAUTICS

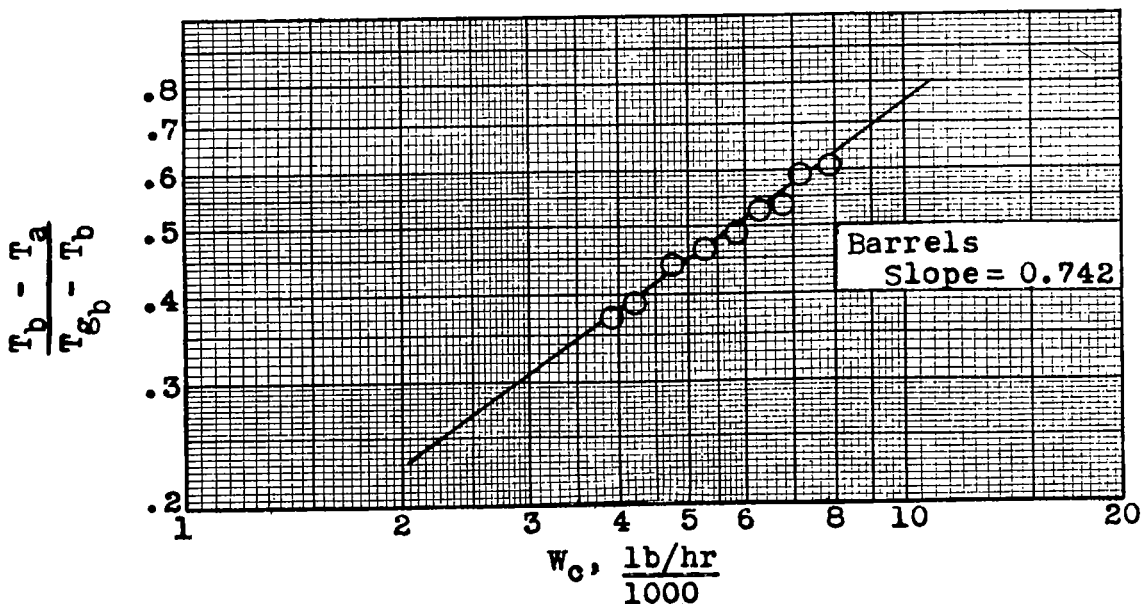


Figure 1. - Variation of $\frac{T_h - T_a}{T_{g_h} - T_h}$ and $\frac{T_b - T_a}{T_{g_b} - T_b}$ with W_o at $\sigma\Delta p$ of 12.2 inches of water for heads and 10.5 inches of water for barrels. Spark advance, 25° B.T.C.

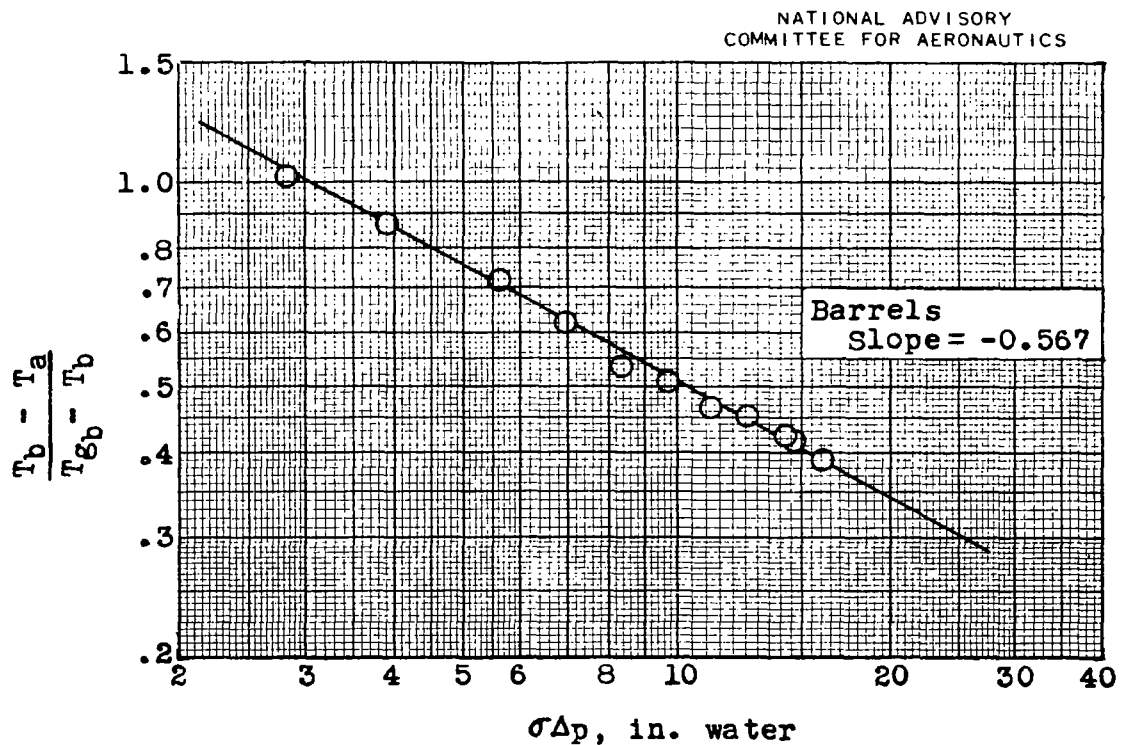
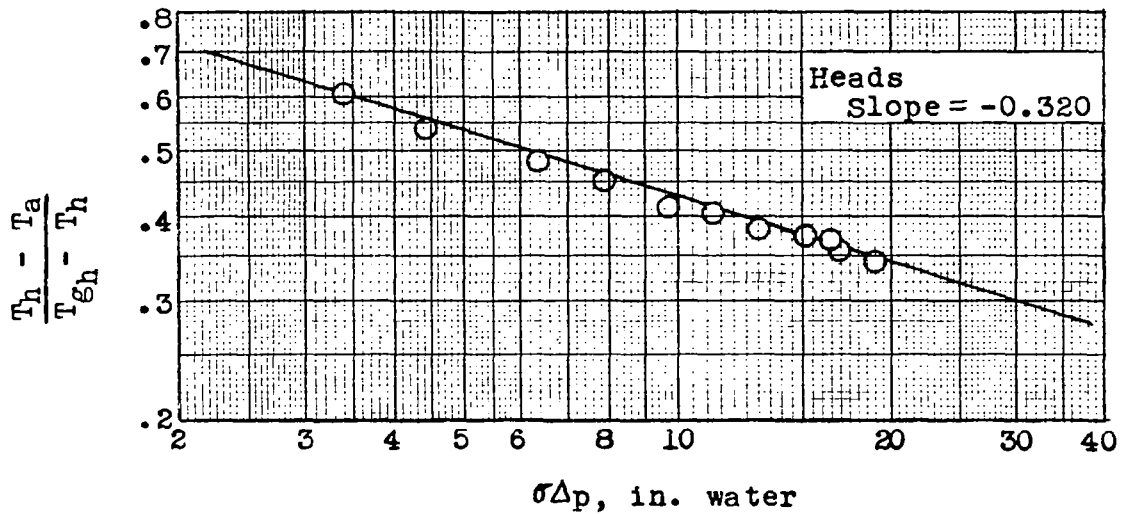


Figure 2. - Variation of $\frac{T_h - T_a}{T_{g_h} - T_h}$ and $\frac{T_b - T_a}{T_{g_b} - T_b}$ with $\sigma \Delta p$ at a w_c of 5590 pounds per hour. Spark advance, 25° B.T.C.

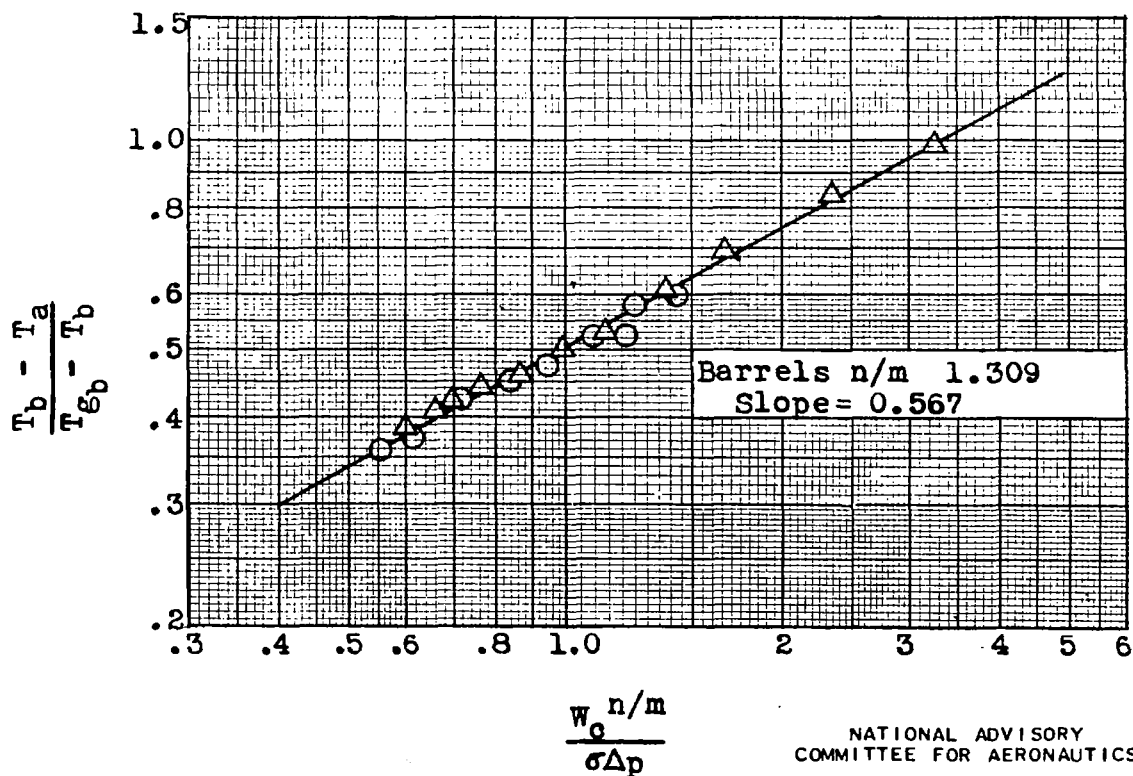
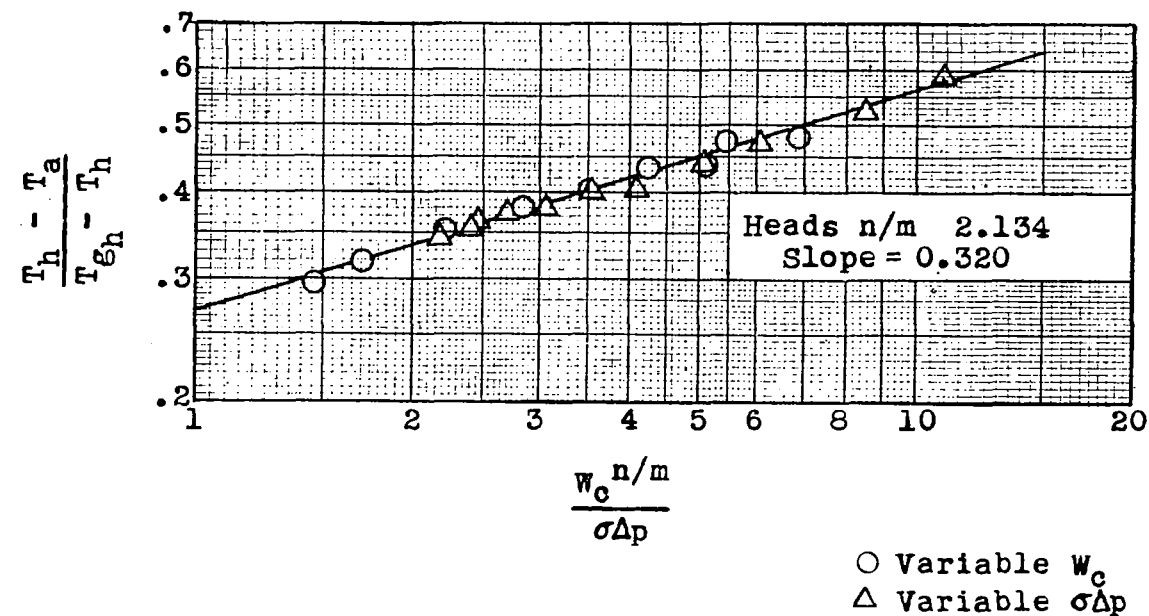


Figure 3. - Cooling-correlation curve at a spark advance of 25° B.T.C.

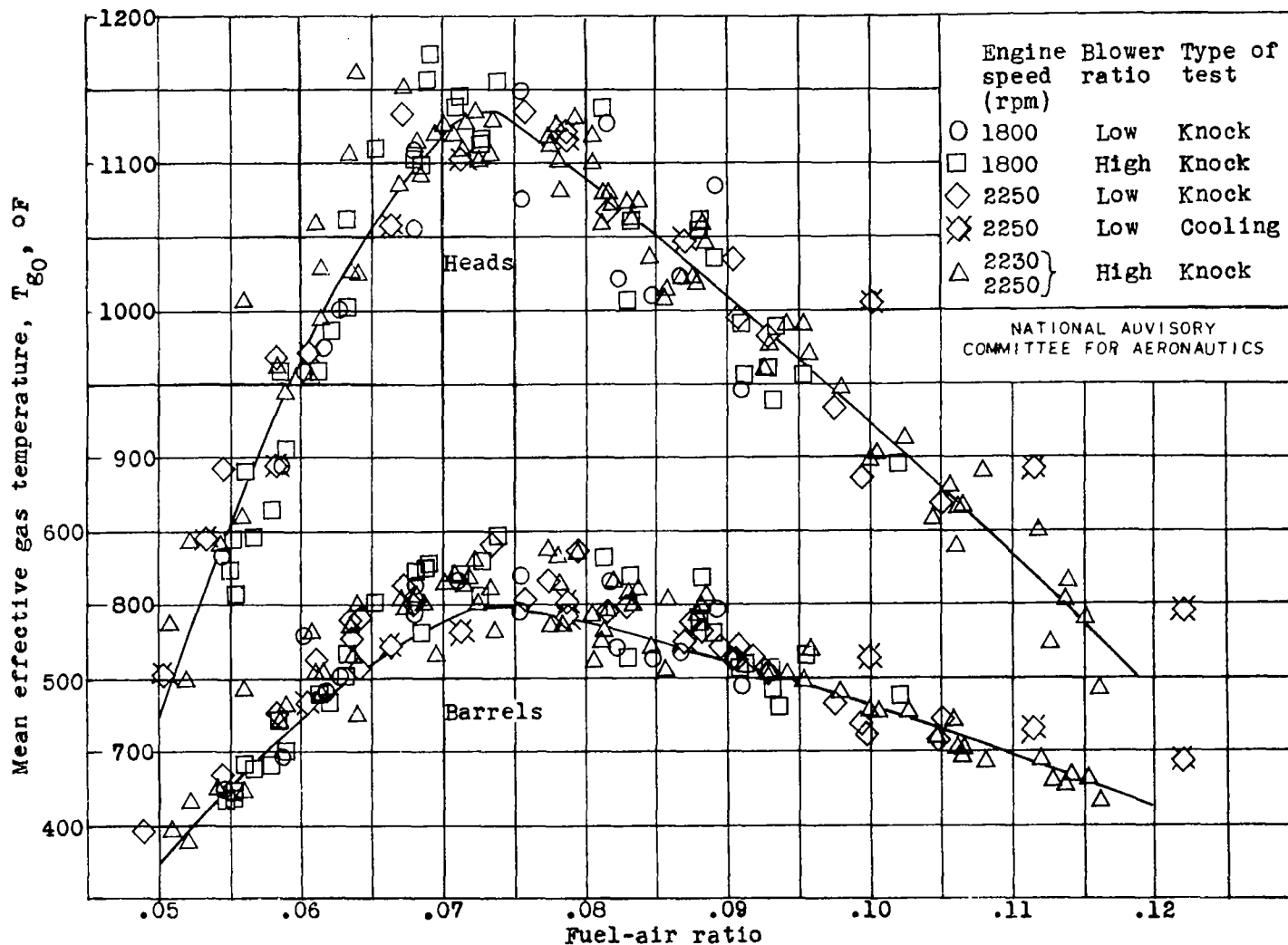


Figure 4. - Variation of mean effective gas temperature T_{g_0} with fuel-air ratio. Engine speed, 1800 to 2250 rpm; spark advance, 25° B.T.C.; high and low blower ratio; carburetor-air temperature, 80° and 100° F; cooling data for 28-R fuel and knock data for 28-R, triptane blend, and xylydine blend fuels.

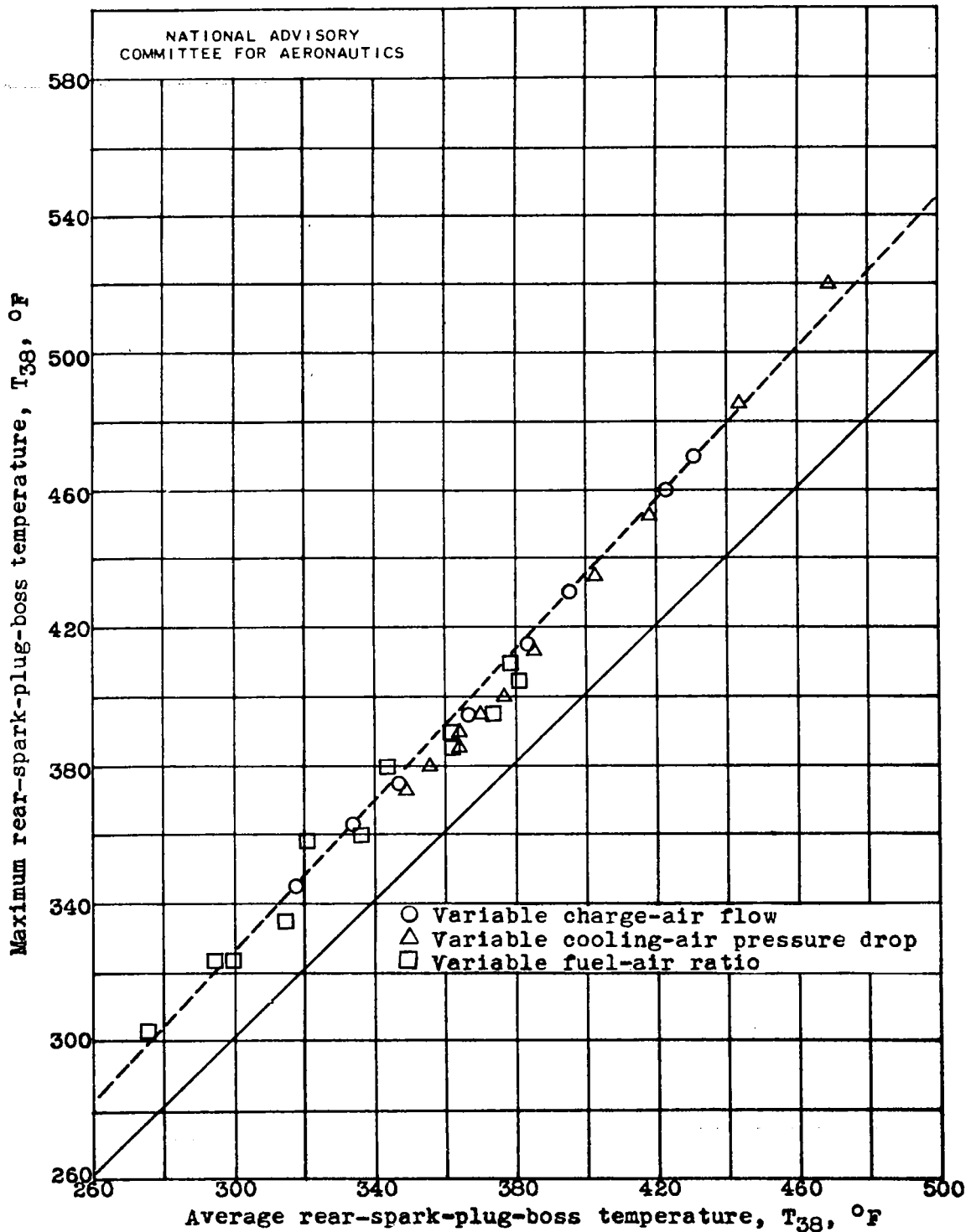


Figure 5. - Deviation of maximum from average rear-spark-plug-boss temperature measured by embedded thermocouples.

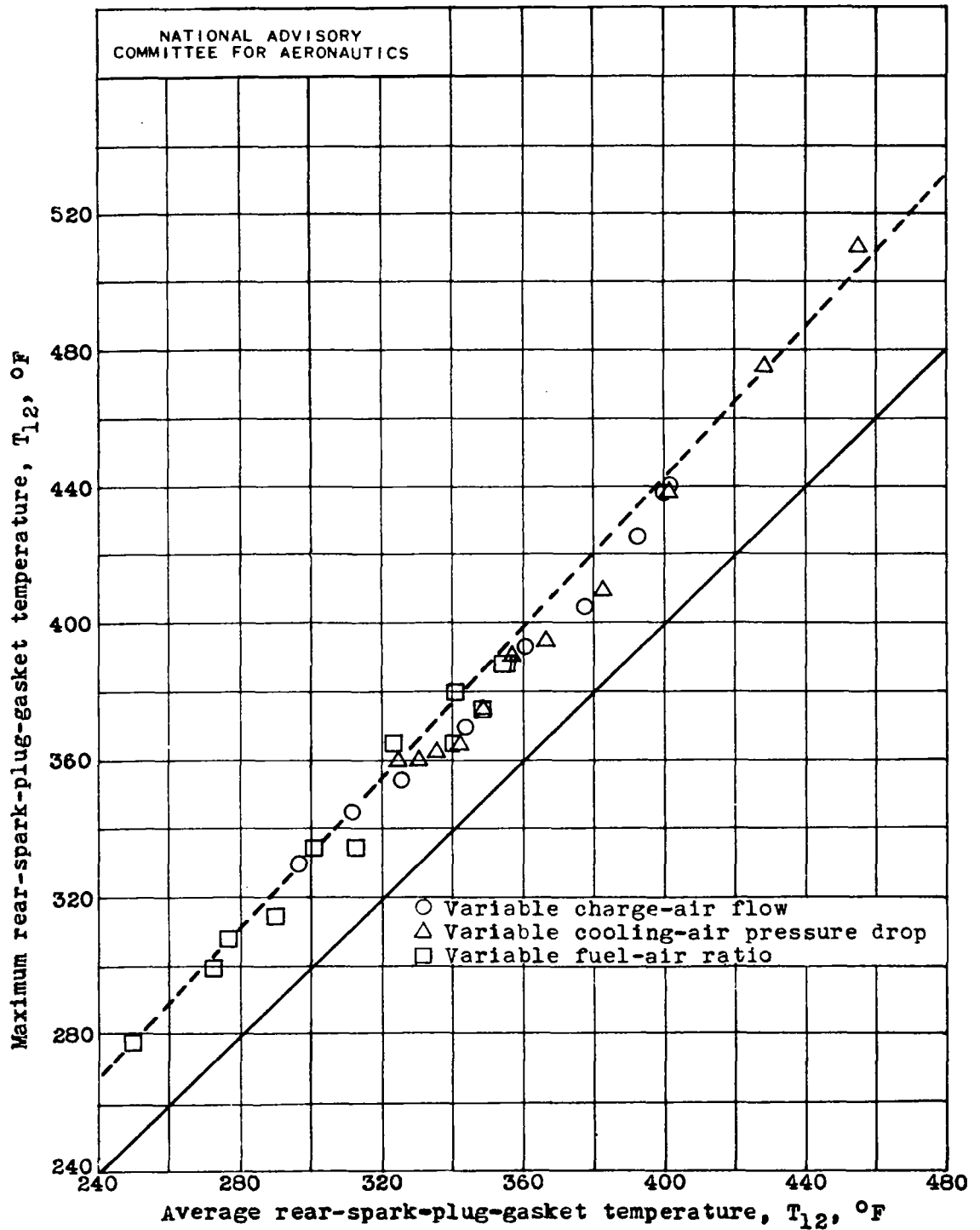


Figure 6. - Deviation of maximum from average rear-spark-plug-gasket temperature.

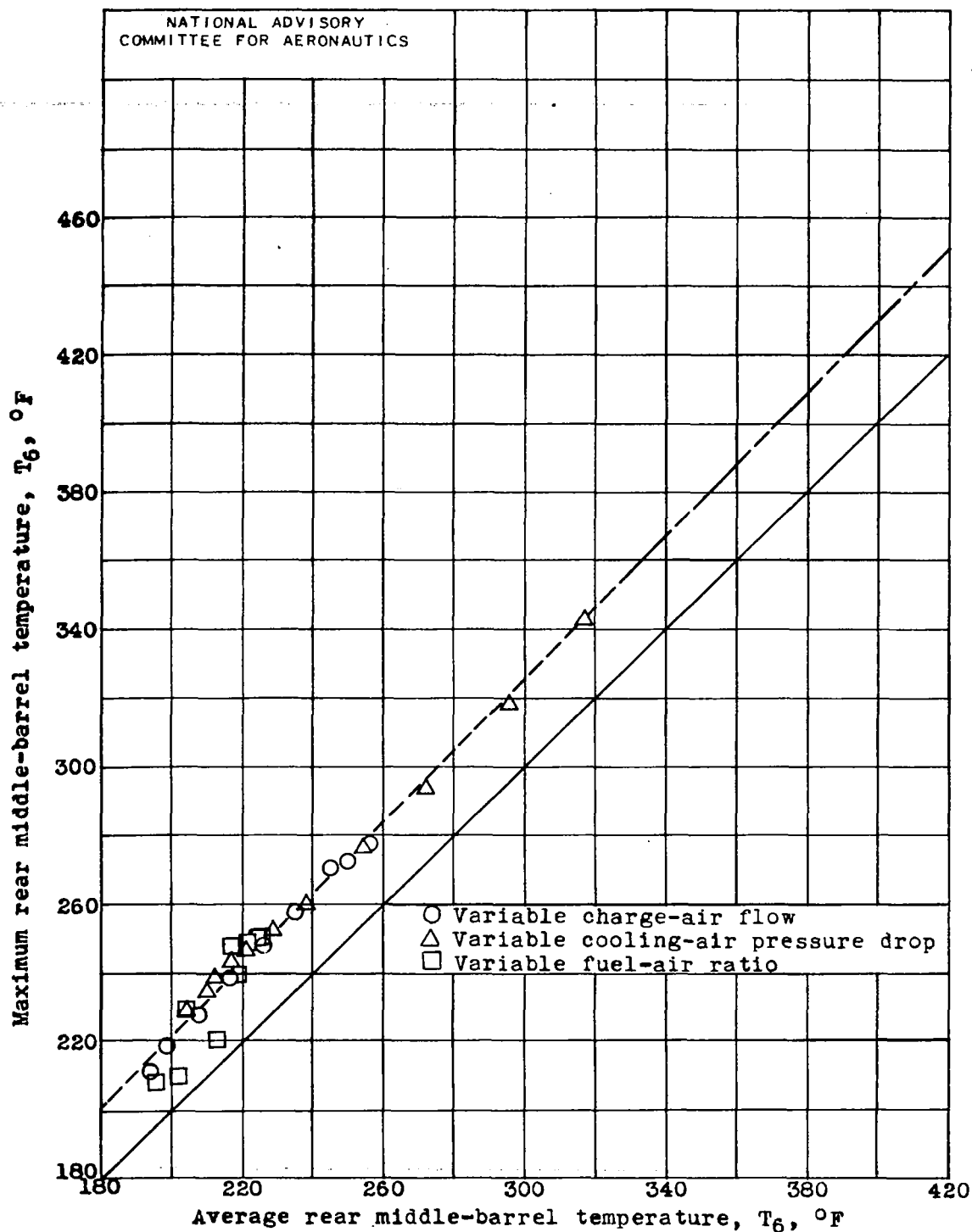


Figure 7. - Deviation of maximum from average rear middle-barrel temperature.

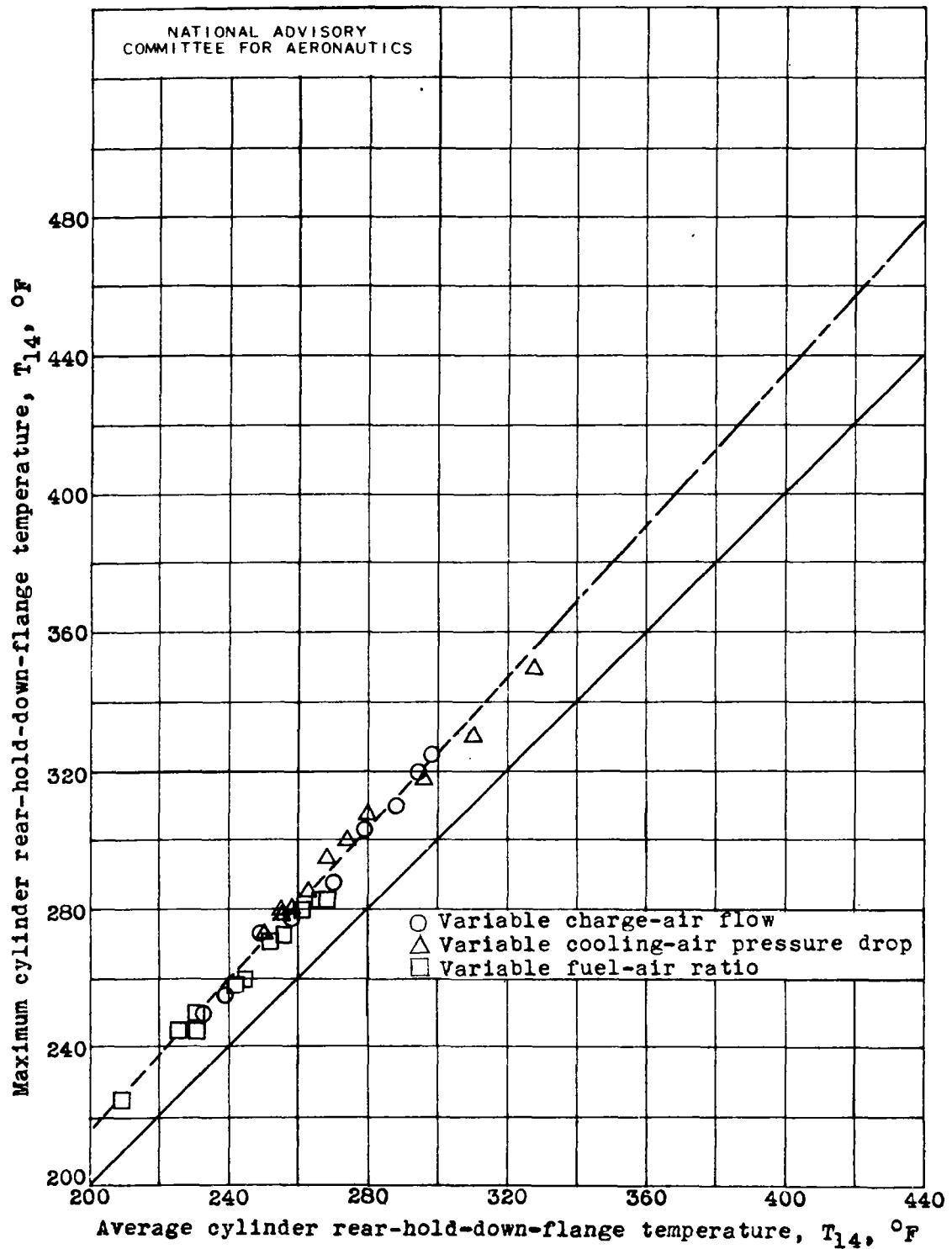


Figure 8. - Deviation of maximum from average cylinder rear-hold-down-flange temperature.

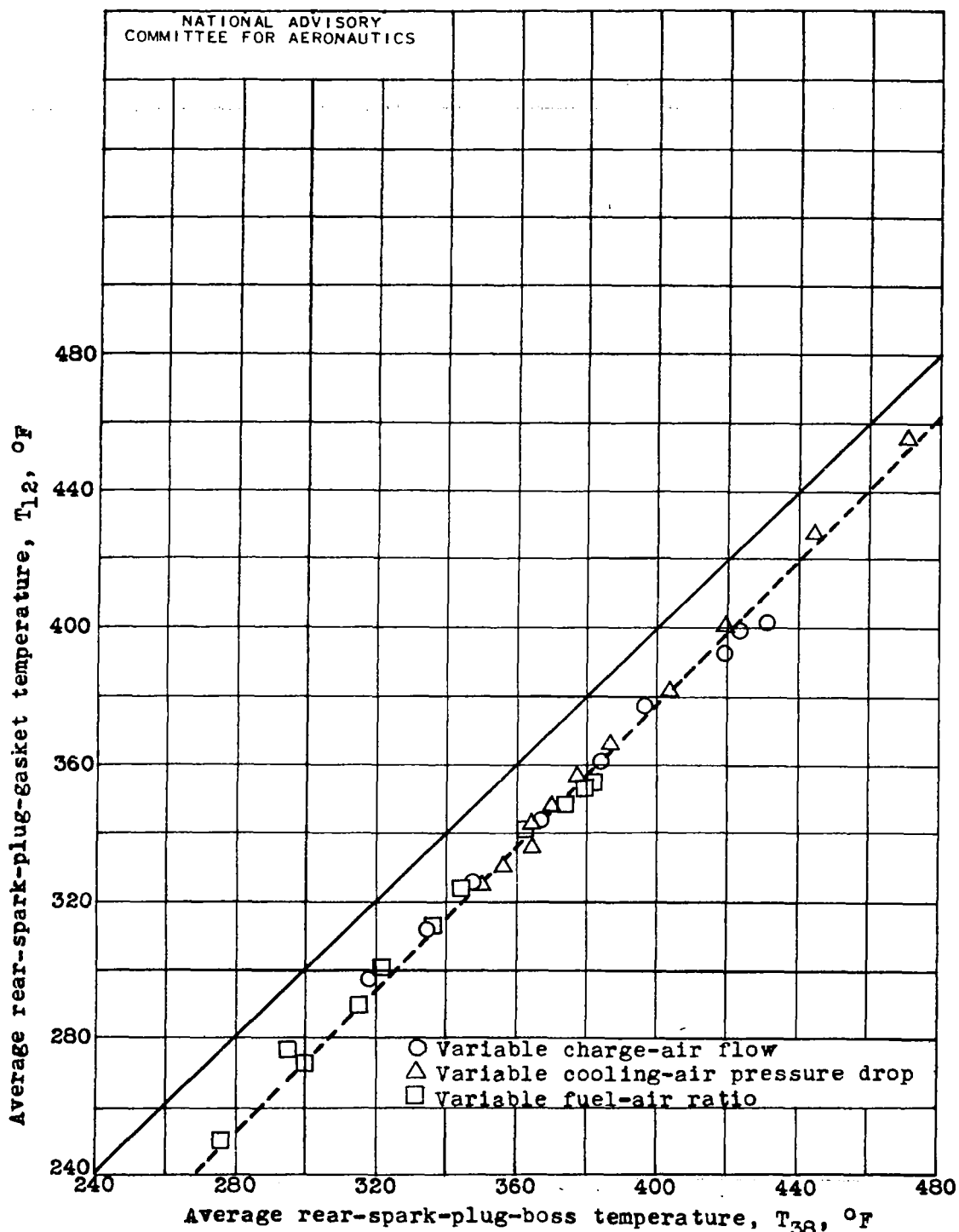


Figure 9. - Comparison of average rear-spark-plug-gasket temperature with average rear-spark-plug-boss temperature.

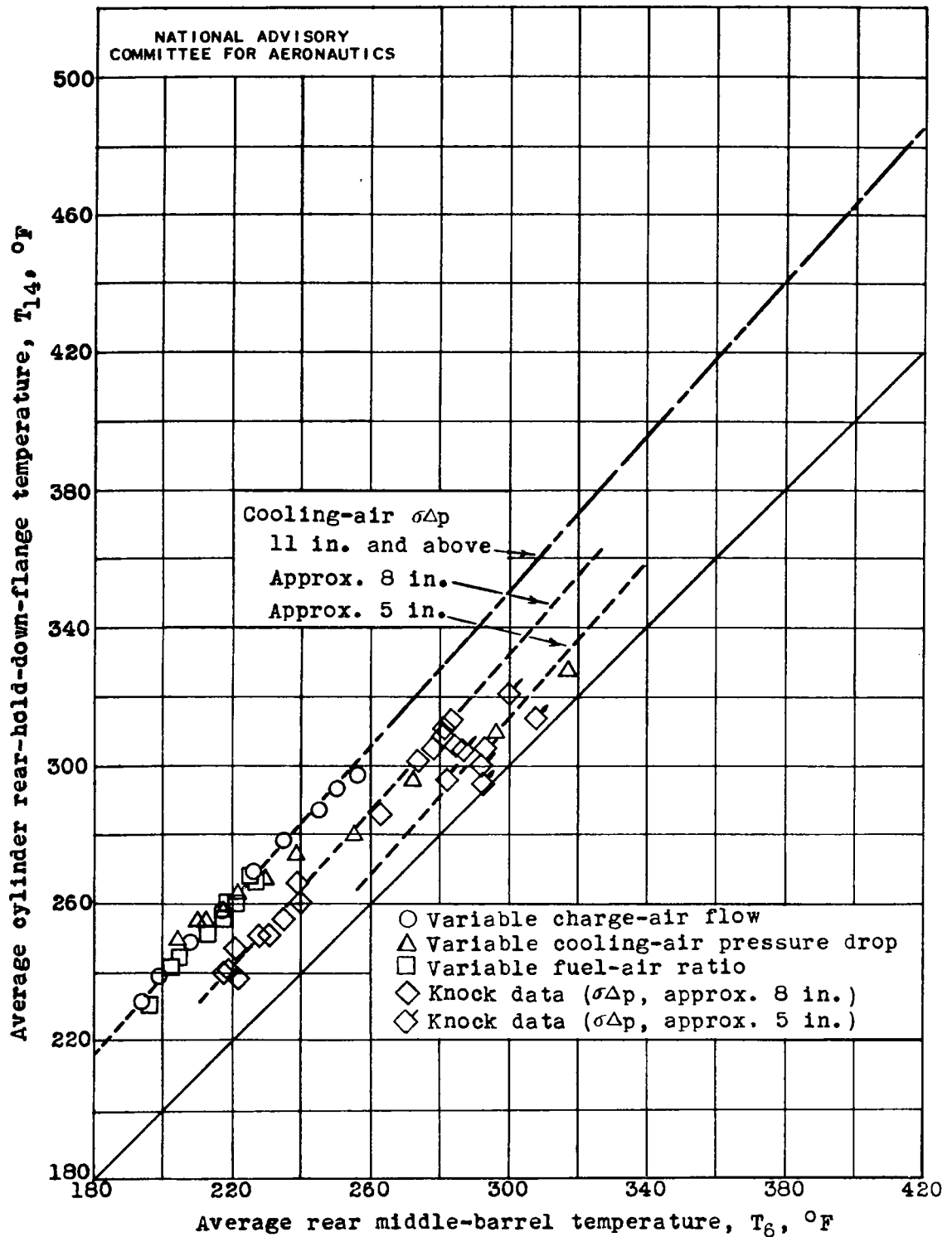


Figure 10. - Comparison of average cylinder rear-hold-down-flange temperature with average rear middle-barrel temperature.

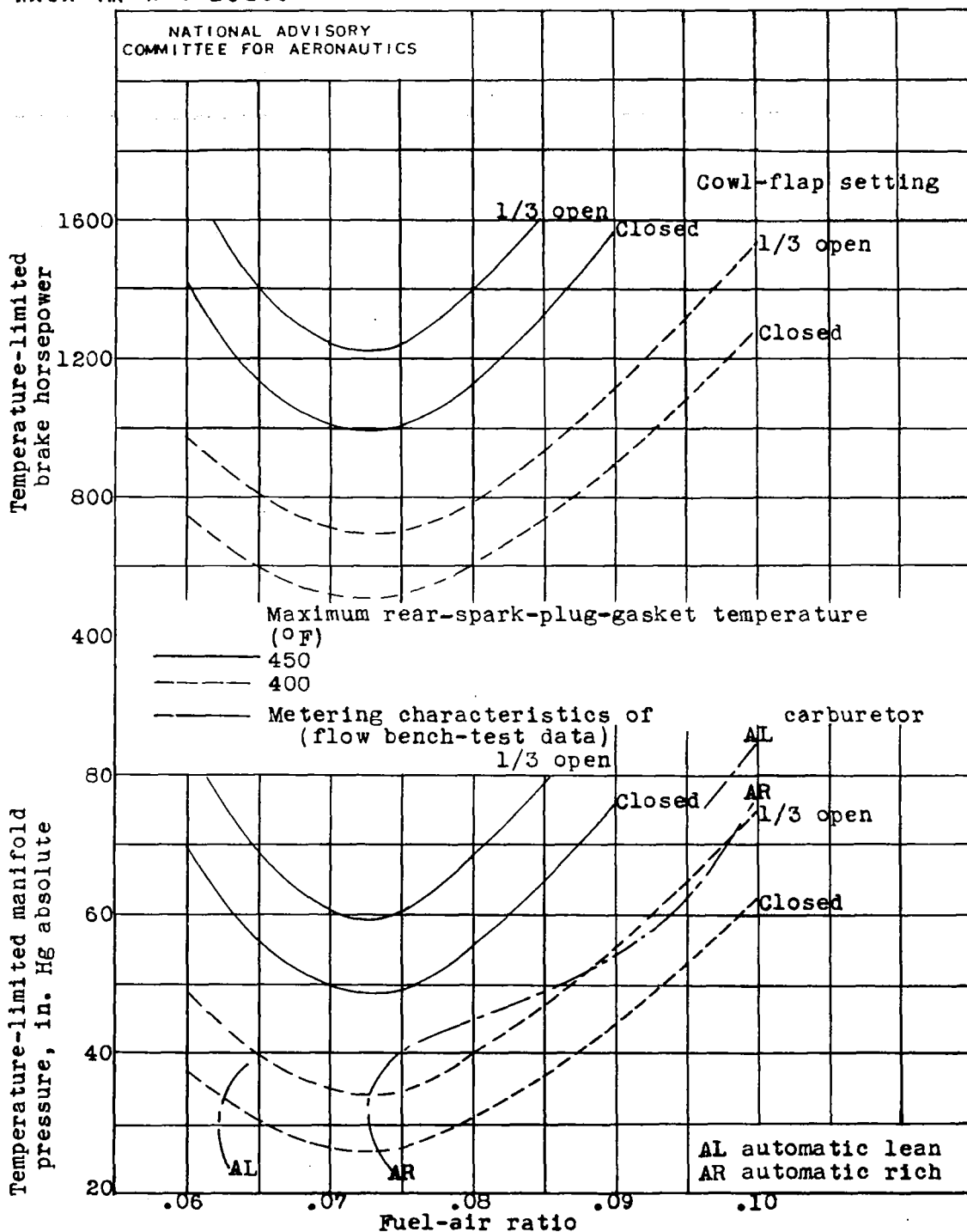


Figure 11. - Predicted temperature-limited brake horsepower and manifold pressure of four modified test engines in four-engine airplane with maximum rear-spark-plug-gasket temperatures of 400° and 450° F and an engine speed of 1800 rpm. Carburetor-air temperature, 85° F; free-air temperature, 60° F; altitude, 7000 feet; low blower ratio; spark advance, 25° B.T.C.

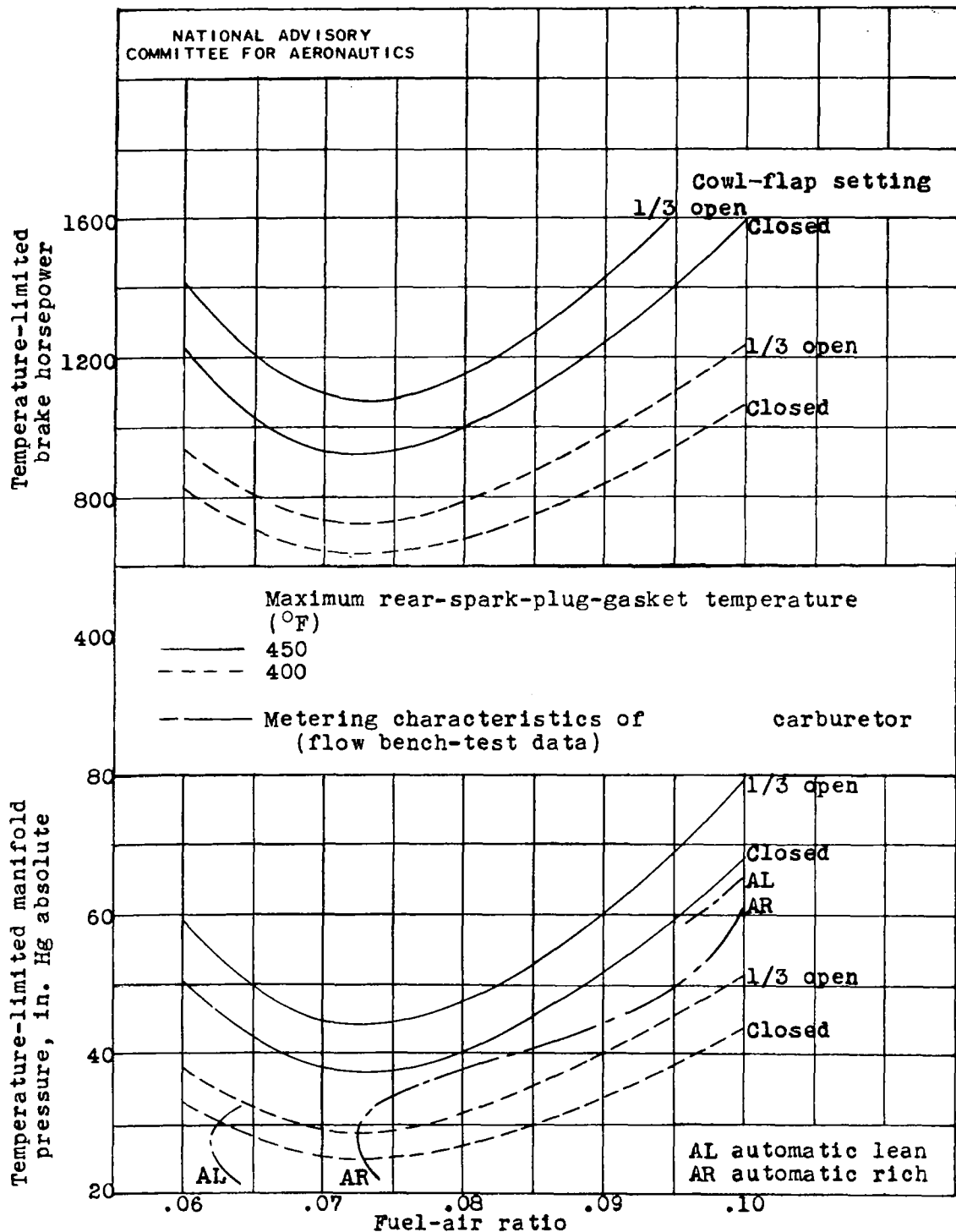


Figure 12. - Predicted temperature-limited brake horsepower and manifold pressure of four modified test engines in four-engine airplane with maximum rear-spark-plug-gasket temperatures of 400° and 450° F and an engine speed of 2250 rpm. Carburetor-air temperature, 85° F; free-air temperature, 60° F; altitude, 7000 feet; low blower ratio; spark advance, 25° B.T.C.

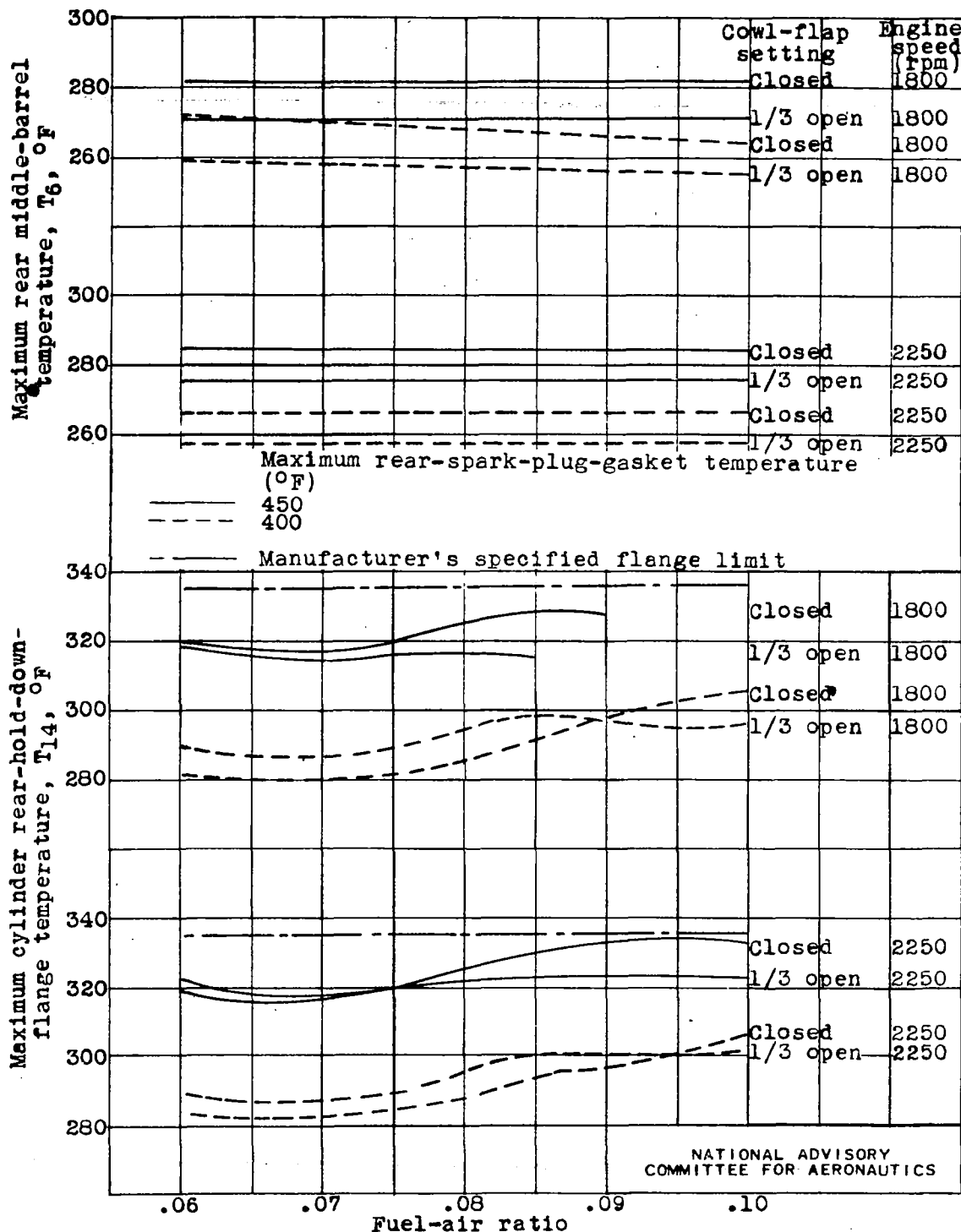


Figure 13. - Predicted maximum rear middle-barrel and cylinder rear-hold-down-flange temperatures for engine speeds of 1800 and 2250 rpm, corresponding to temperature-limited performance curves in figures 11 and 12. Carburetor-air temperature, 85° F; free-air temperature, 60° F; altitude, 7000 feet; low blower ratio; spark advance, 25° B.T.C.

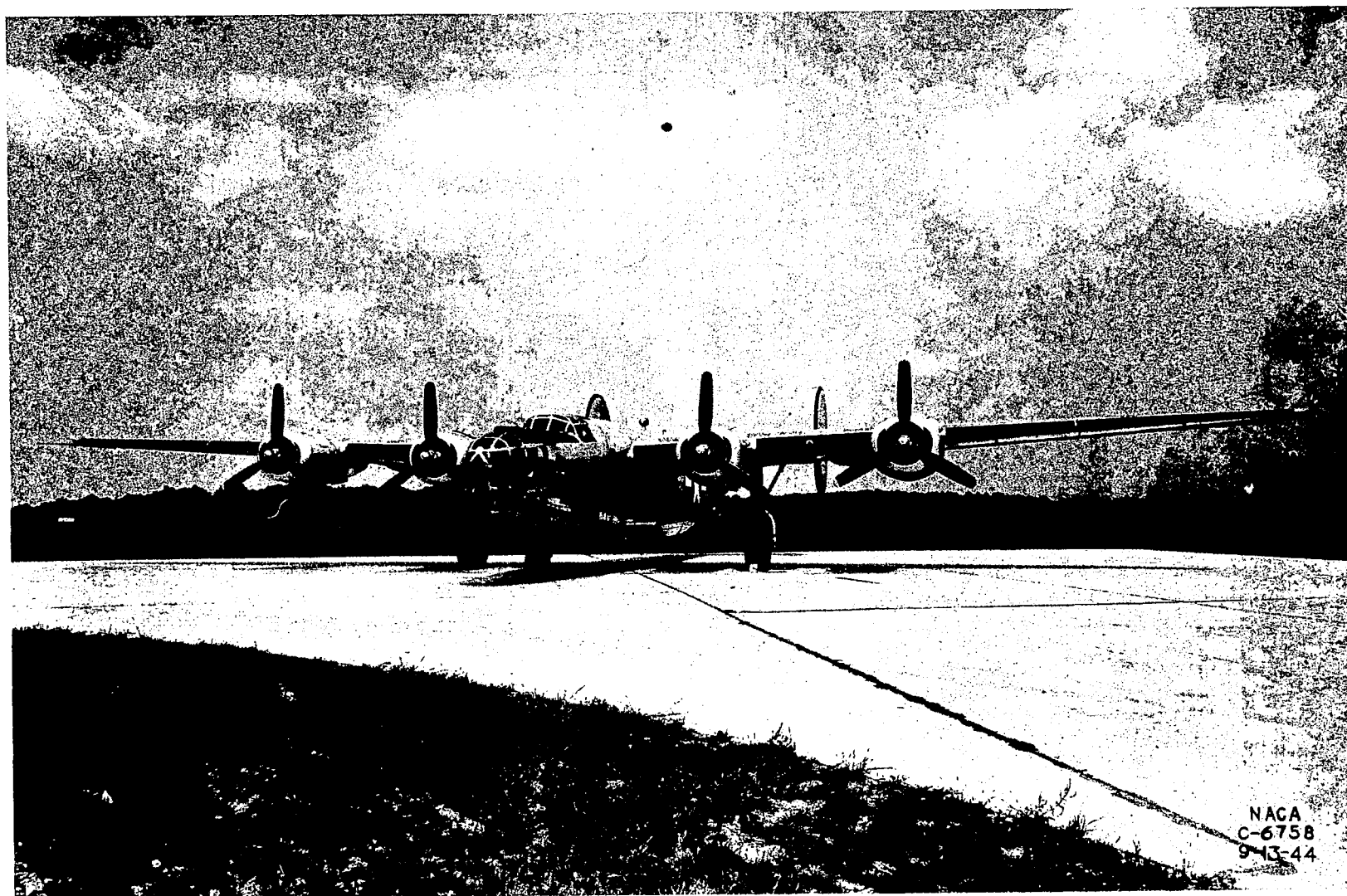
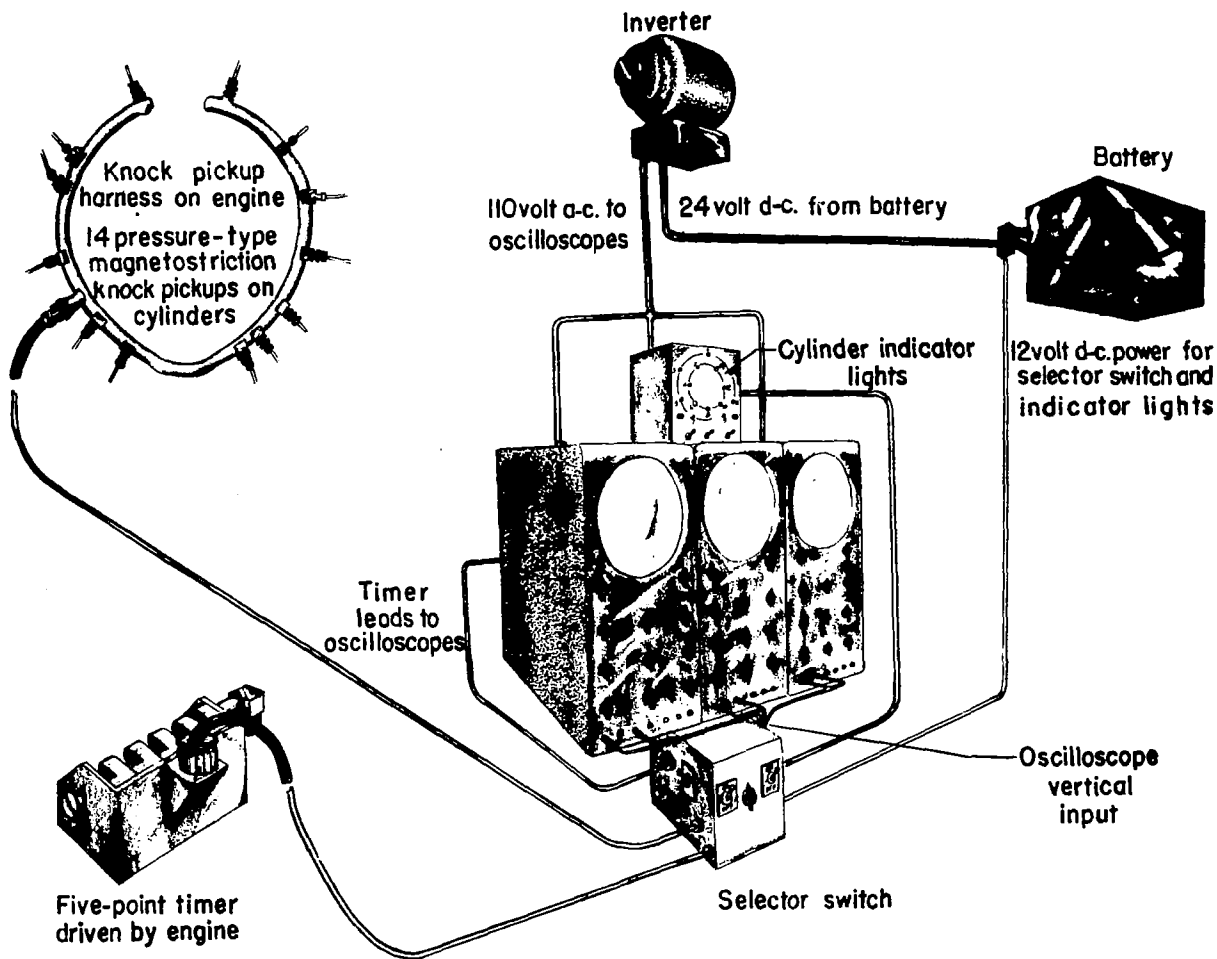
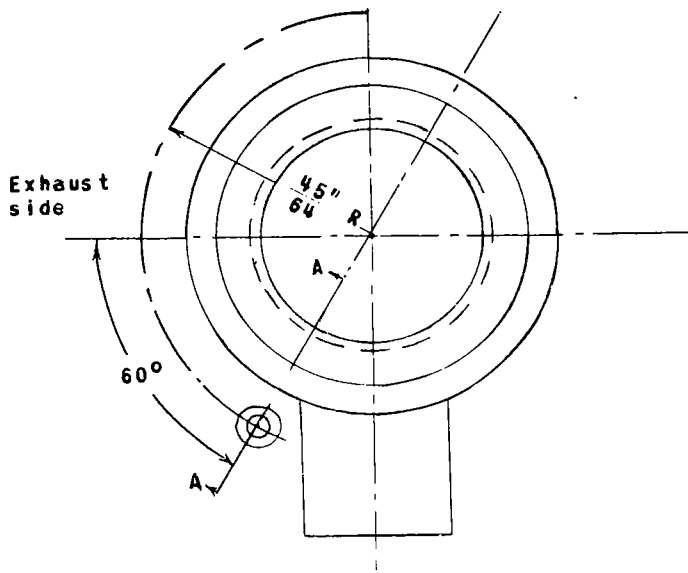


Figure 14. - View of four-engine airplane used for flight knock and cooling investigation.

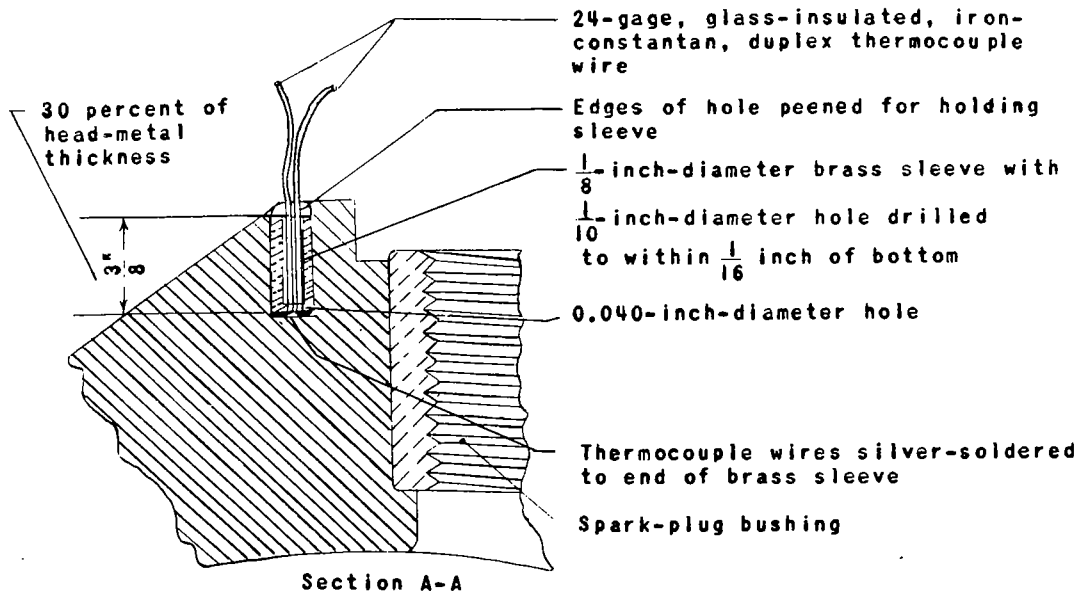


NATIONAL ADVISORY
COMMITTEE FOR AERONAUTICS

Figure 15. - Schematic diagram of knock-detection system.



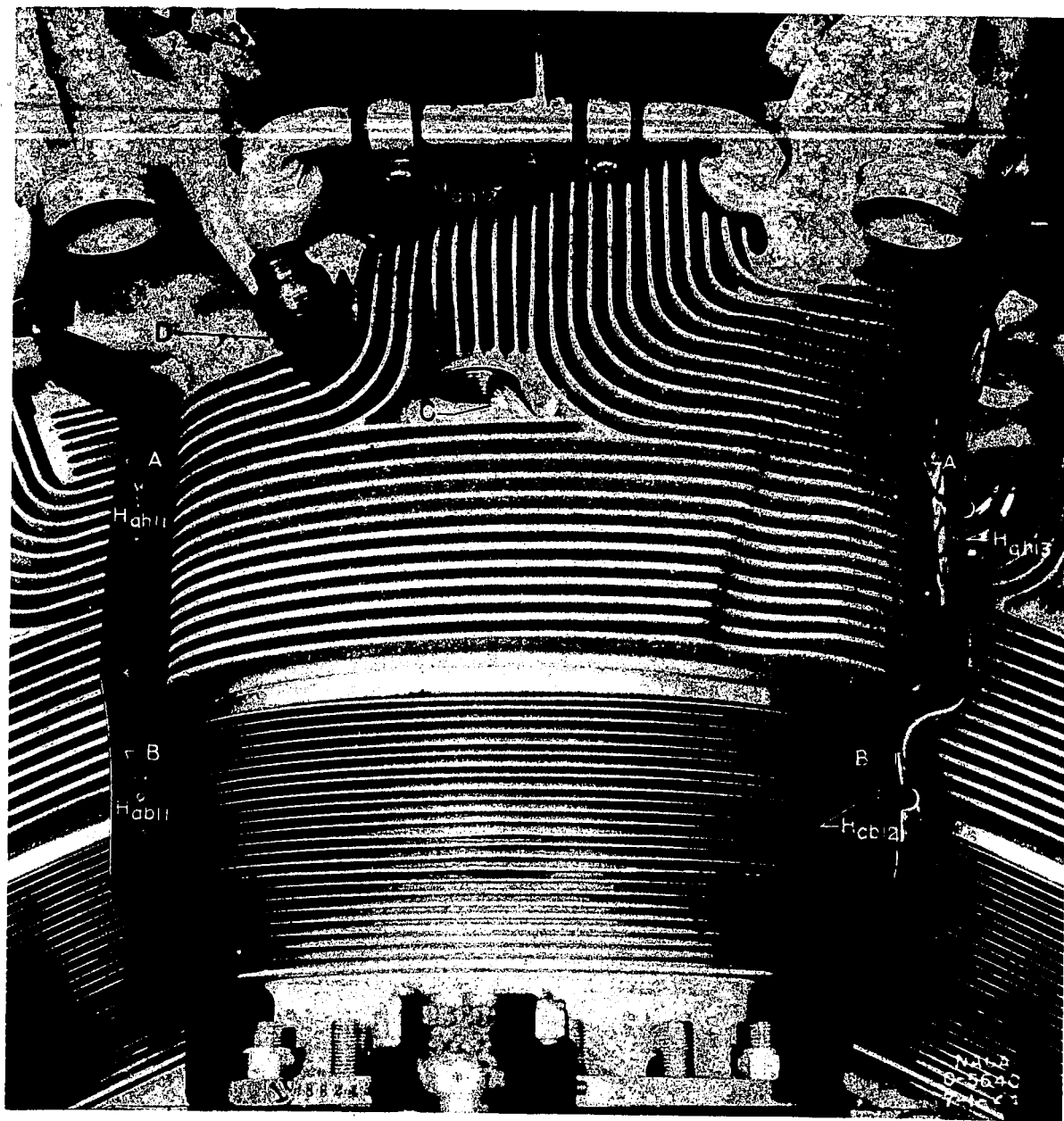
(a) Method of locating thermocouple.



(b) Method of installing thermocouple.

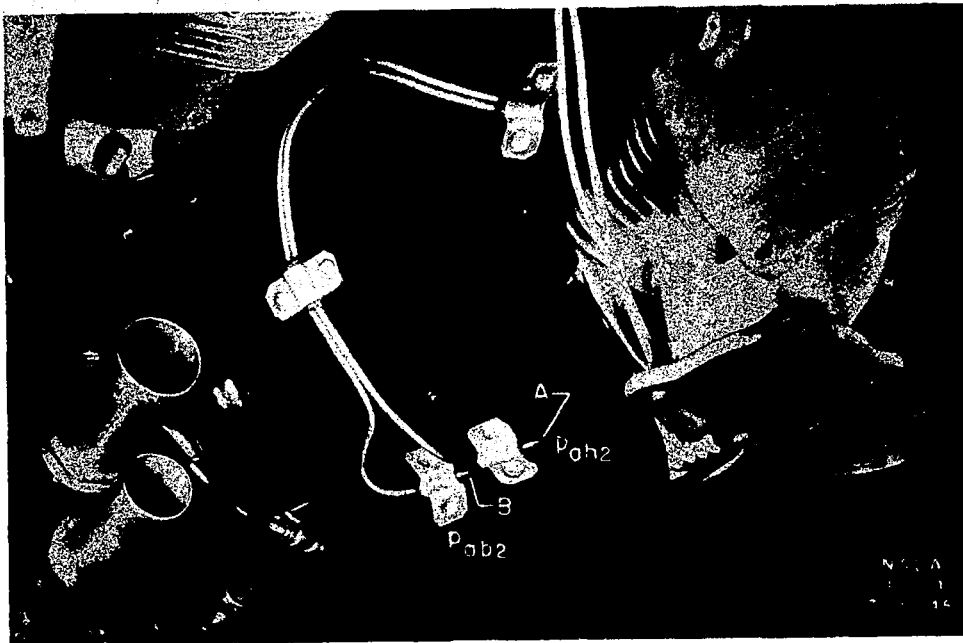
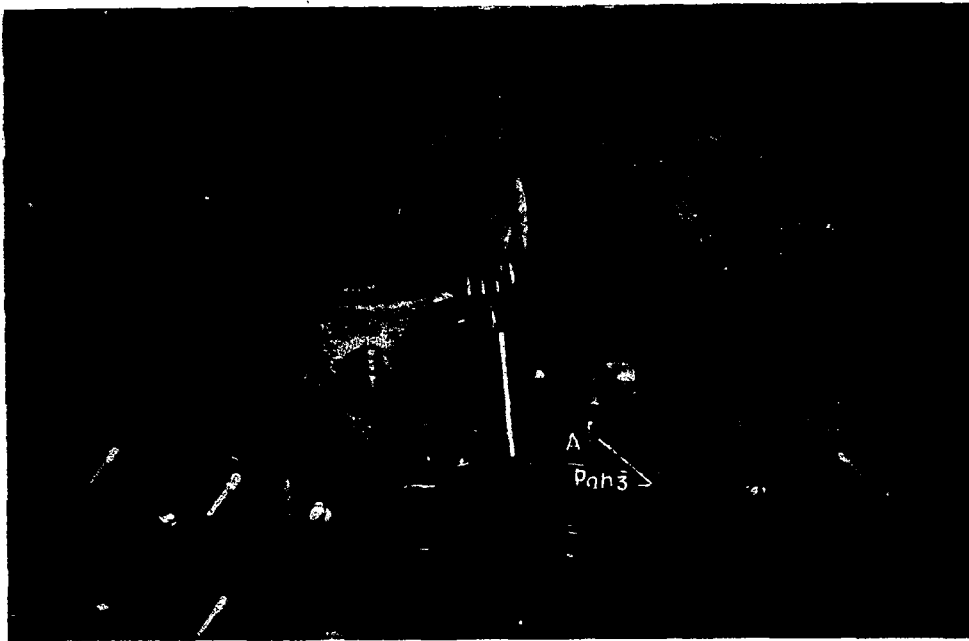
NATIONAL ADVISORY
COMMITTEE FOR AERONAUTICS

Figure 16. - Methods of locating and installing embedded thermocouple T_{38} in rear-spark-plug boss on cylinder head of modified test engine.



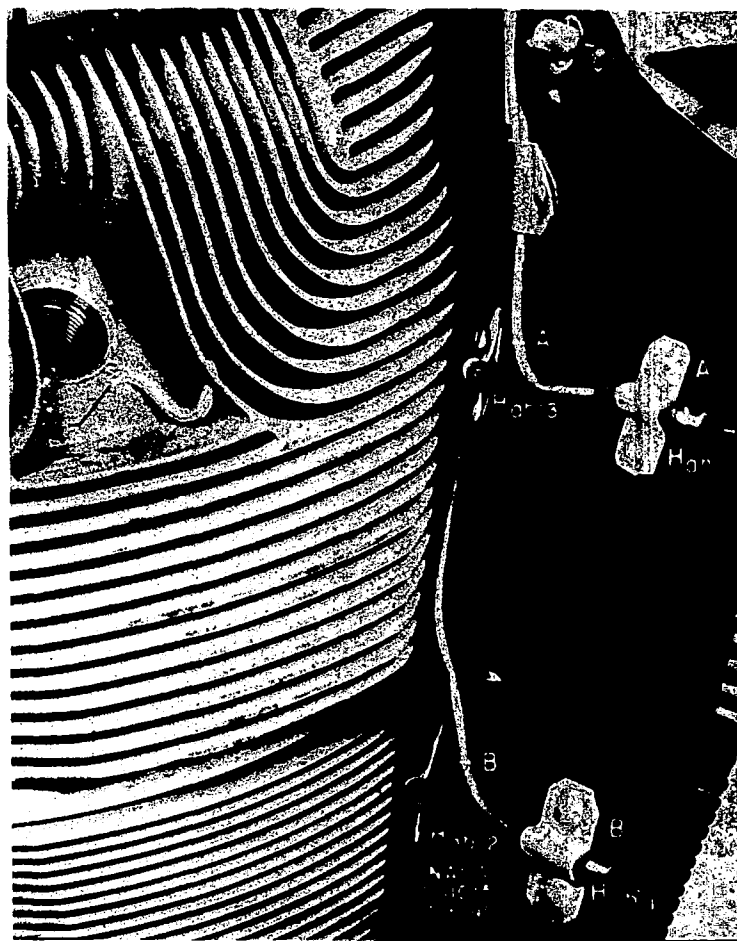
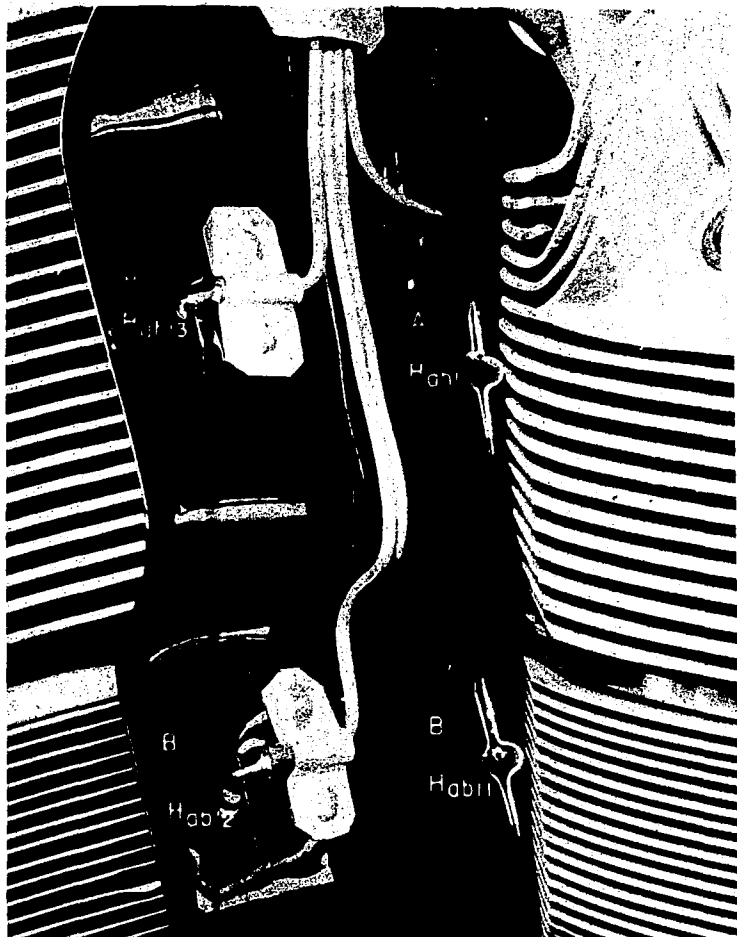
- A Total-pressure tubes at baffle inlet to head (H_{ah11} , H_{ah12} , H_{ah13})
- B Total-pressure tubes at baffle inlet to barrel (H_{ab11} , H_{ab12})
- C Embedded thermocouple in front-spark-plug boss (T_{36})
- D Pressure-type knock pickup

Figure 17. - Installation of pressure tubes, thermocouple, and knock pickup on front of modified test-engine front-row cylinder.



- A Open end static-pressure tubes behind the top head sealing baffle, rear cylinders only (p_{ah2} , p_{ah3})
- B Open end static-pressure tube in exit curl of baffle, rear cylinders only (p_{ab2})
- C Embedded thermocouple in rear-spark-plug boss (T_{38})

Figure 18. - Pressure-tube installation on top head baffle and in baffle-exit curl of modified test-engine rear-row cylinders, and embedded thermocouple T_{38} .



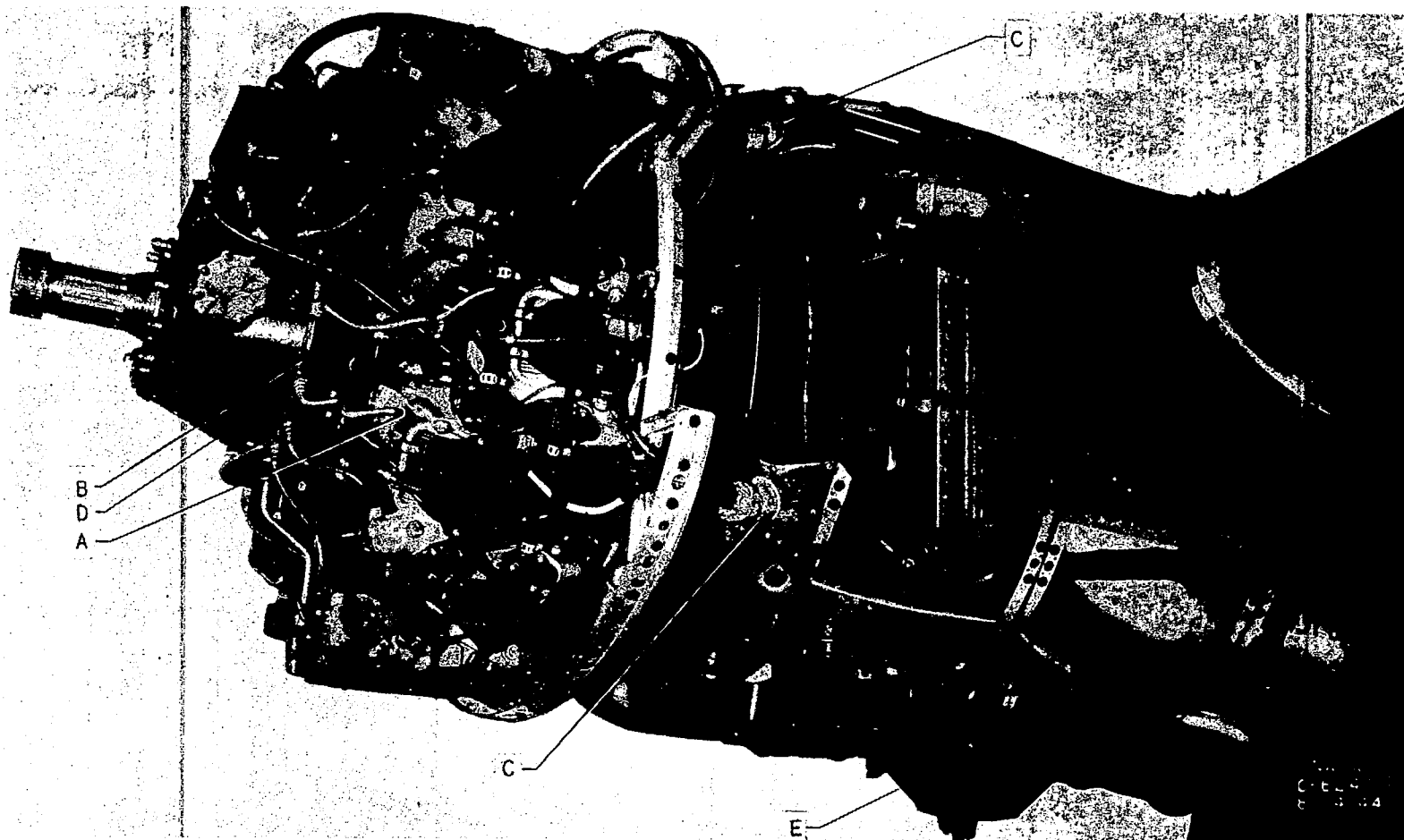
- A Total-pressure tubes at baffle inlet to head (H_{ah11} , H_{ah13})
- B Total-pressure tubes at baffle inlet to barrel (H_{ab11} , H_{ab12})
- C Embedded thermocouple in front-spark-plug boss (T_{36})

Figure 19. - Installation of pressure tubes and thermocouples on the front of the rear-row cylinders of modified test engine.



- A Rear-spark-plug-gasket thermocouple (T_{12})
- B Rear middle-barrel thermocouple (T_6)
- C Rear-hold-down-flange thermocouple (T_{14})
- D Pressure tubes at baffle exit (p_{ah2} , p_{ab2})

Figure 20. - Rear view of a rear-row cylinder of modified test engine showing general installation of thermocouples and pressure tubes.



- A Knock pickup, front row
- B Knock harness and leads
- C Pressure tubes and thermocouple leads through fire wall
- D Torque nose section with 16:9 reduction gearing
- E Furnace built into exhaust stack for oxidizing exhaust sample

Figure 21. - General view of installation on modified test engine.

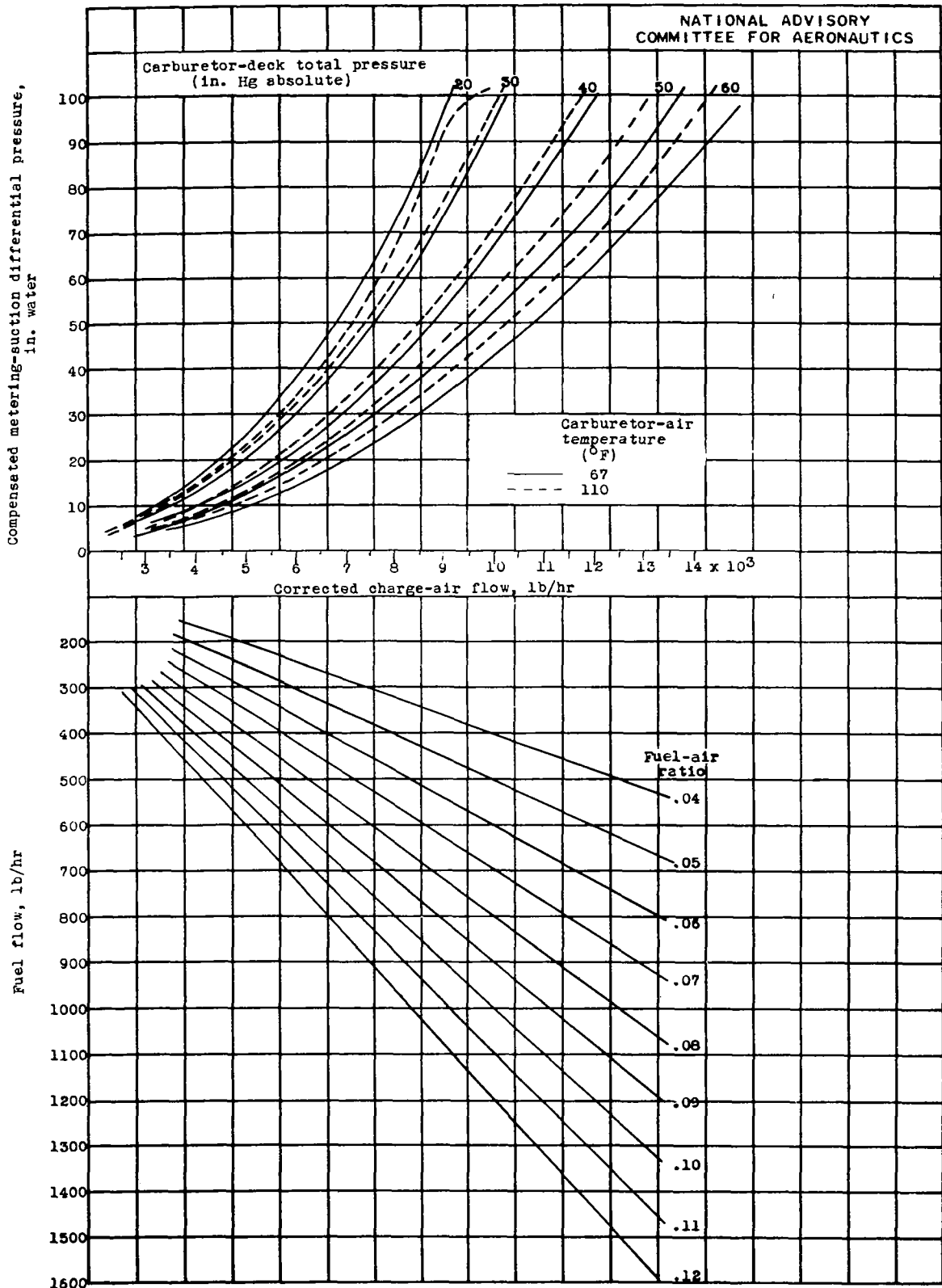
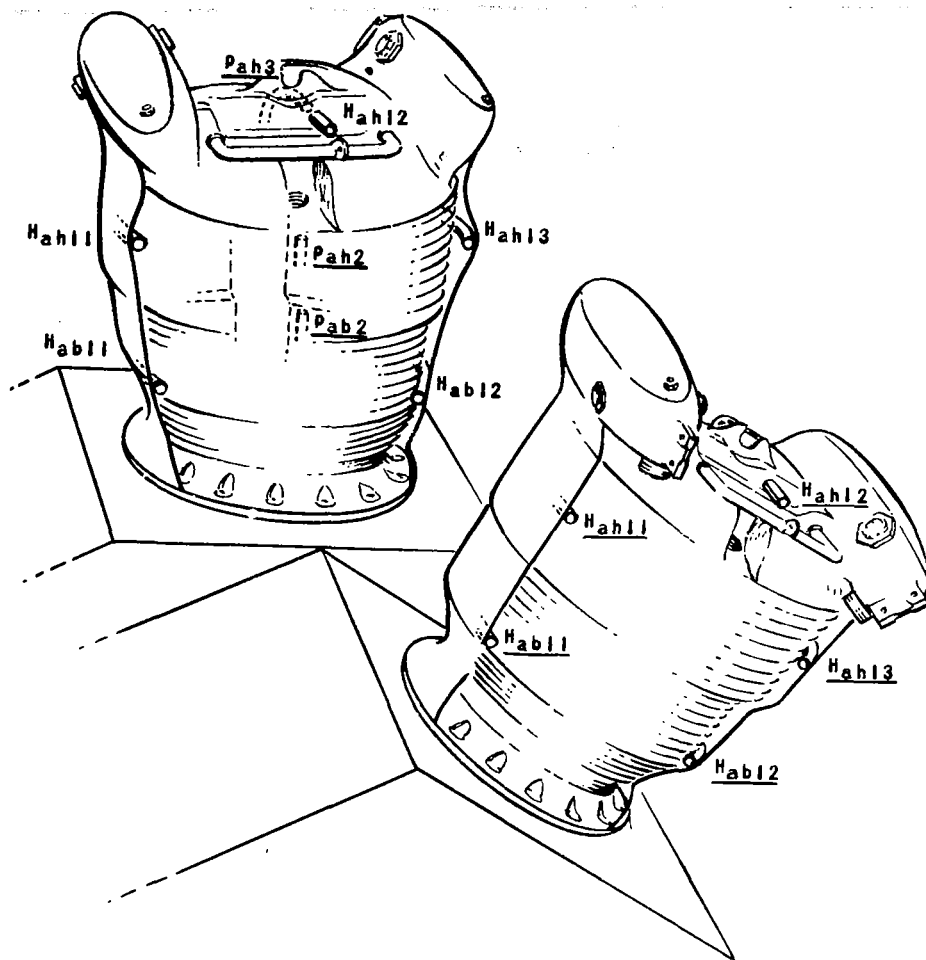
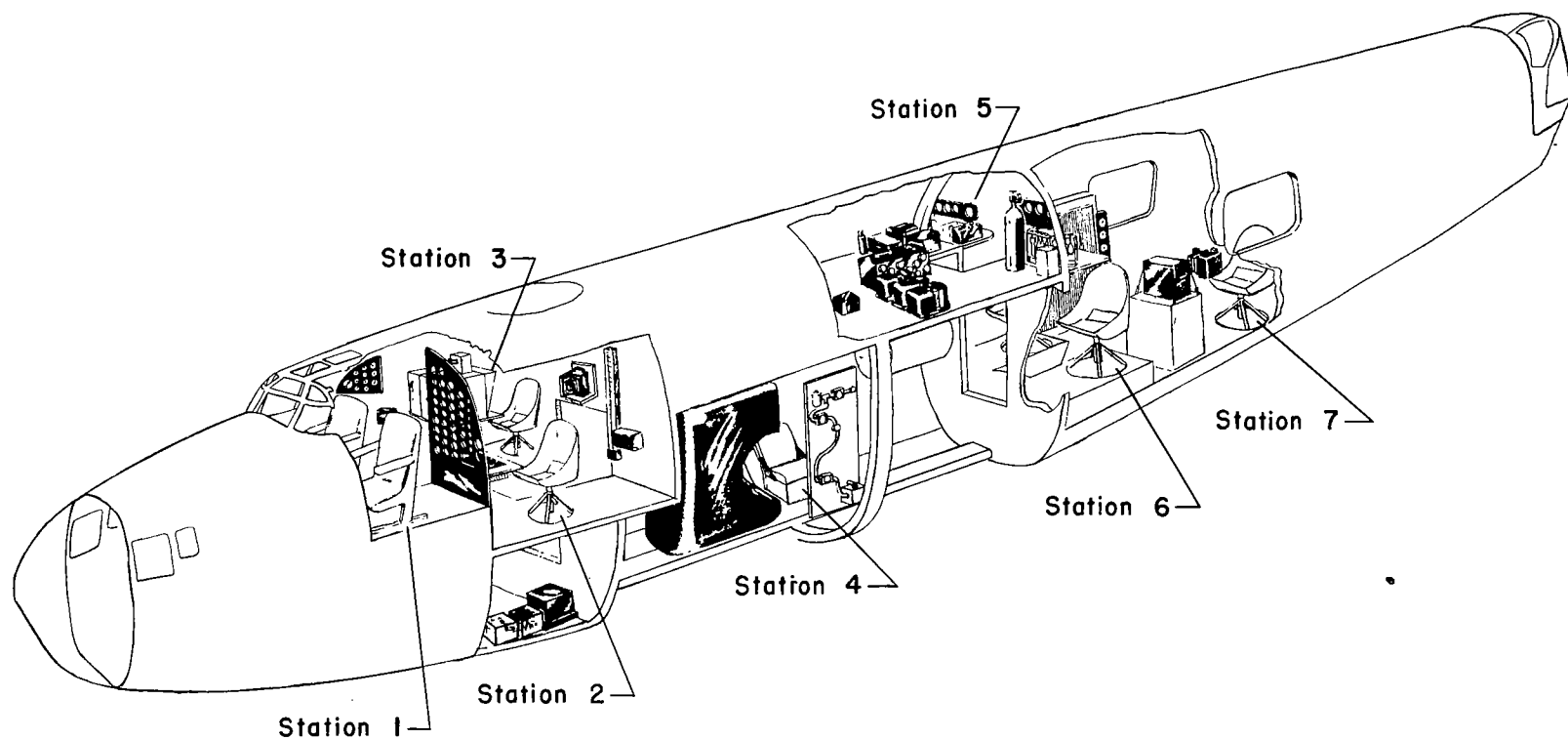


Figure 22. - Chart for determining fuel-air ratios during flight tests.



NATIONAL ADVISORY
COMMITTEE FOR AERONAUTICS

Figure 23. - Schematic diagram of front-row and rear-row cylinder of modified test engine showing location of total (H) and static (p) pressure tubes. Underlined designations represent pressure tubes used in determination of Δp for correlation equation.



NATIONAL ADVISORY
COMMITTEE FOR AERONAUTICS

Figure 24. - Location of airplane stations and of test instrumentation in four-engine airplane.

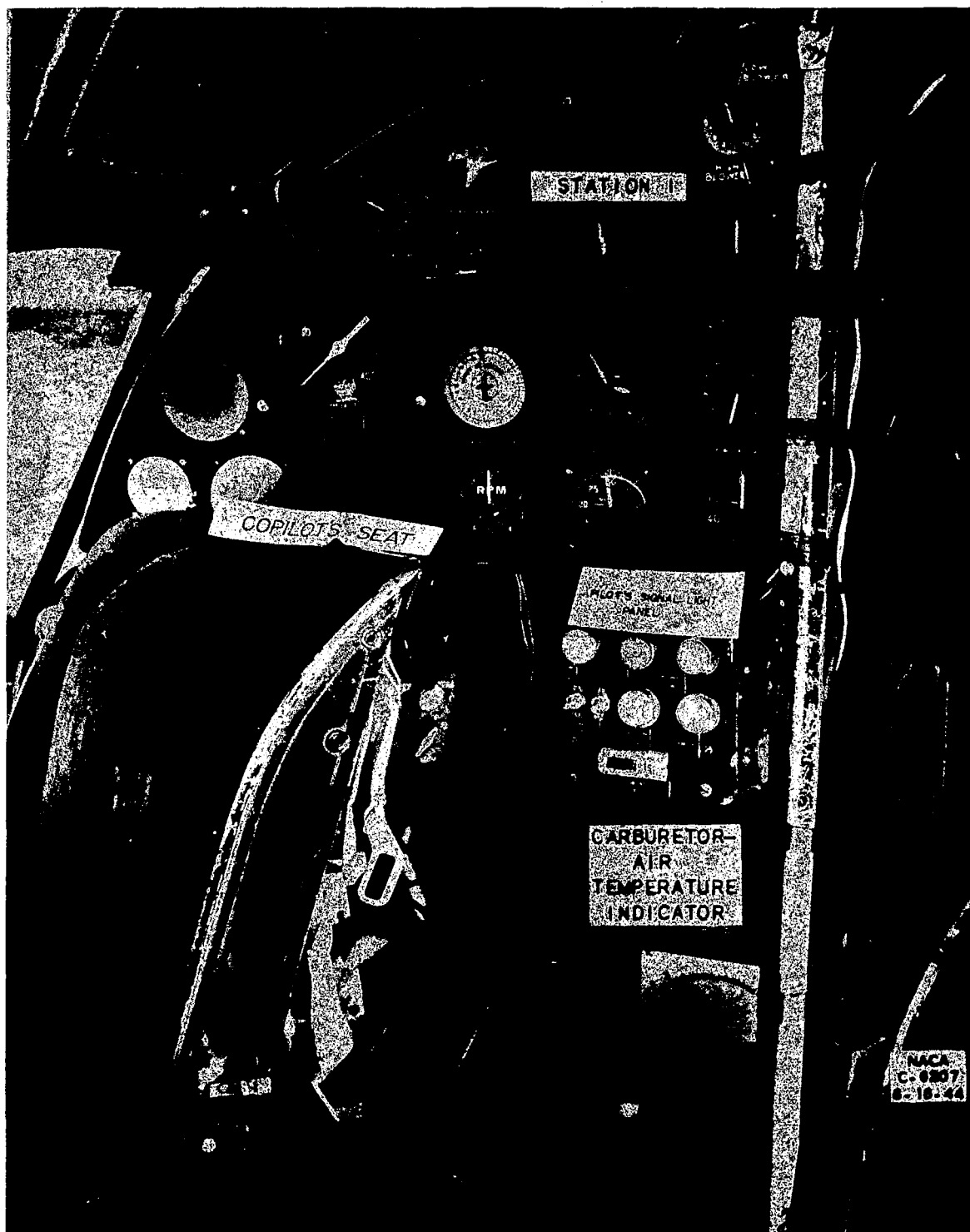


Figure 25. - Station I. Pilot's station showing panel board of special instruments for test engine, carburetor-air-temperature indicator, and signal lights.

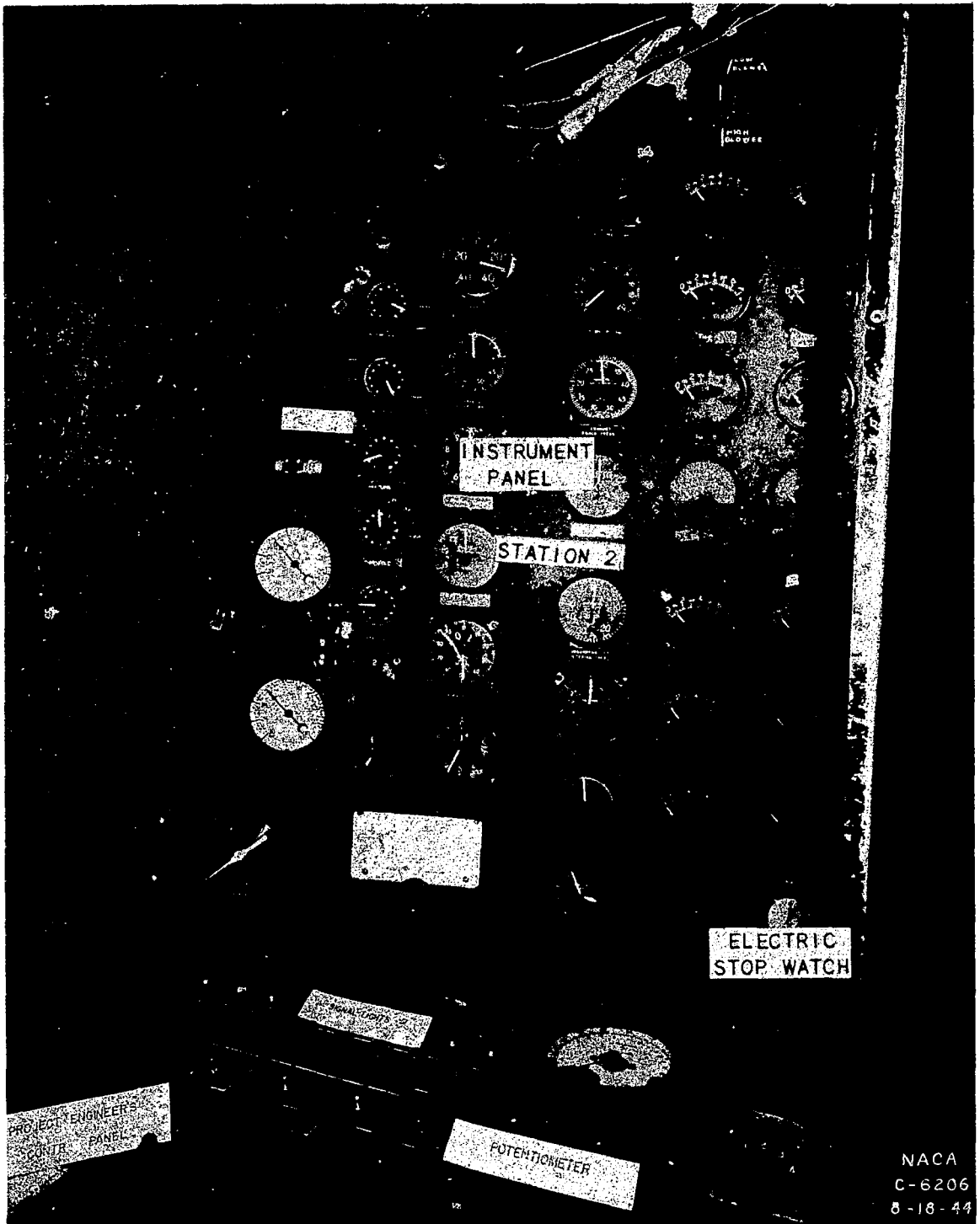


Figure 26. - Station 2. Engineer's instrument panel for test engine and airplane, signal system for contact with other stations, and controls for special recording instruments.

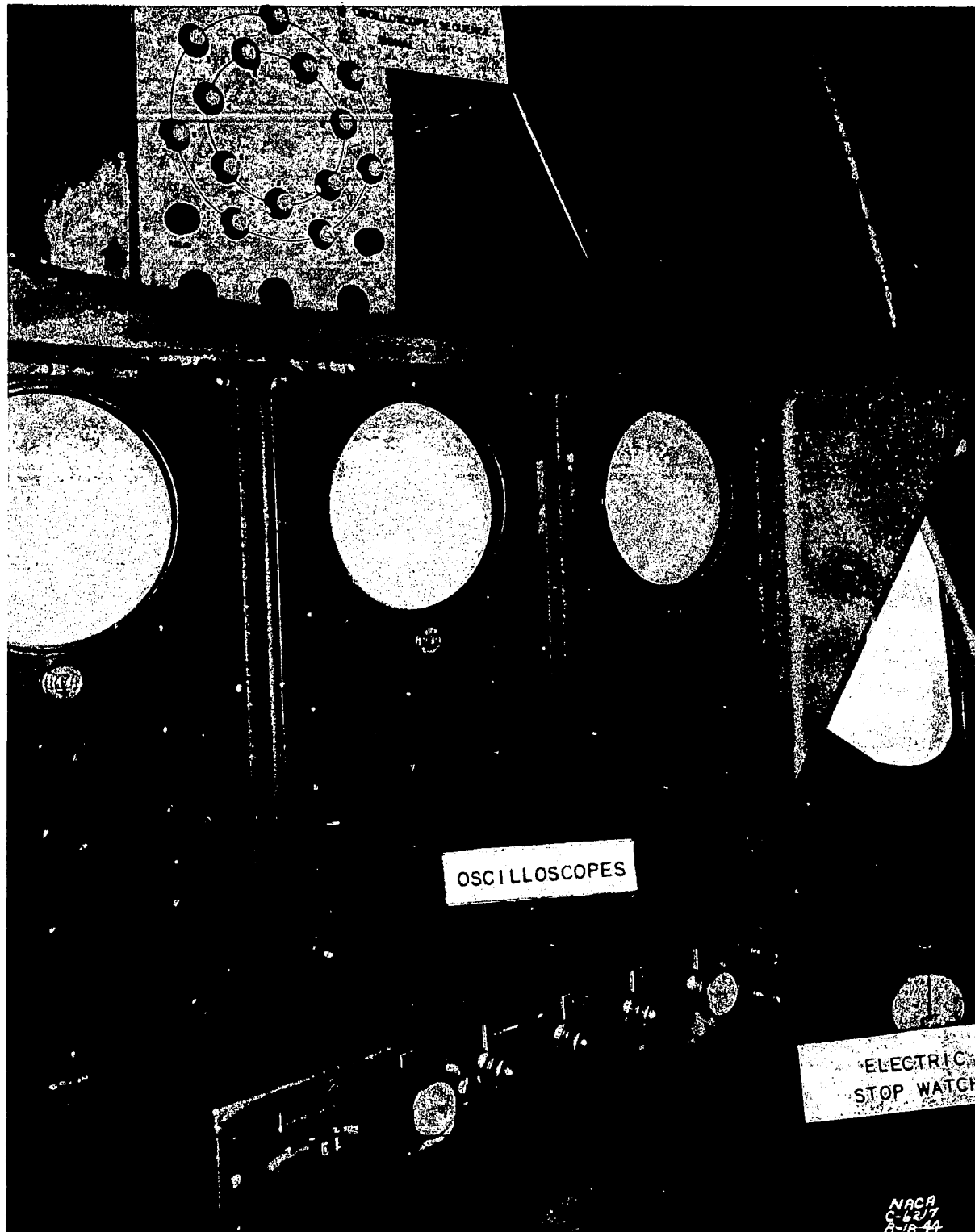


Figure 27. - Station 3. Oscilloscopes for observation of knock, cylinder sequence signal lights, stop watch, and station ready lights.

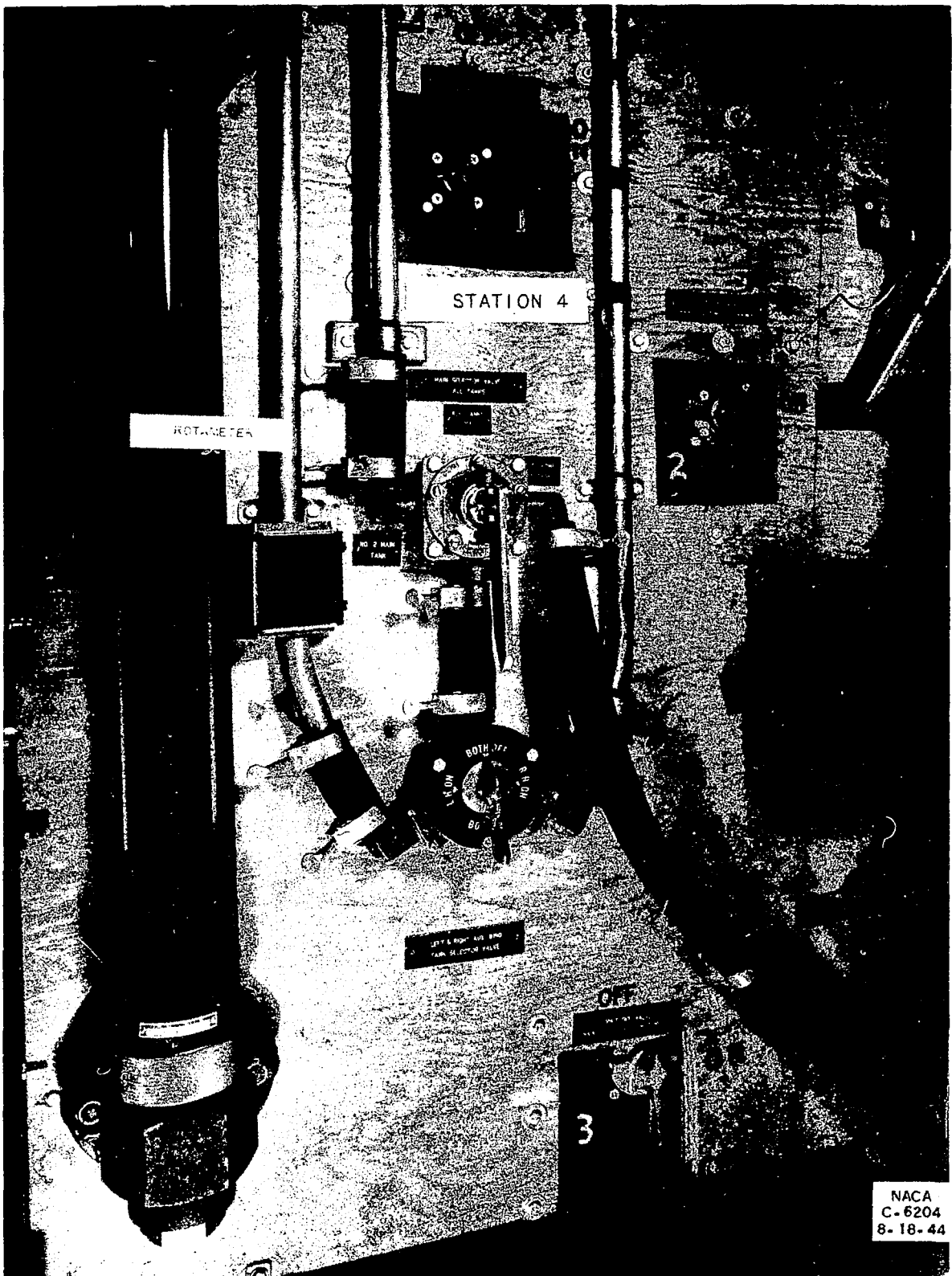


Figure 28. - Station 4. Fuel selection panel in rear bomb bay showing rotameter for measuring fuel flow.

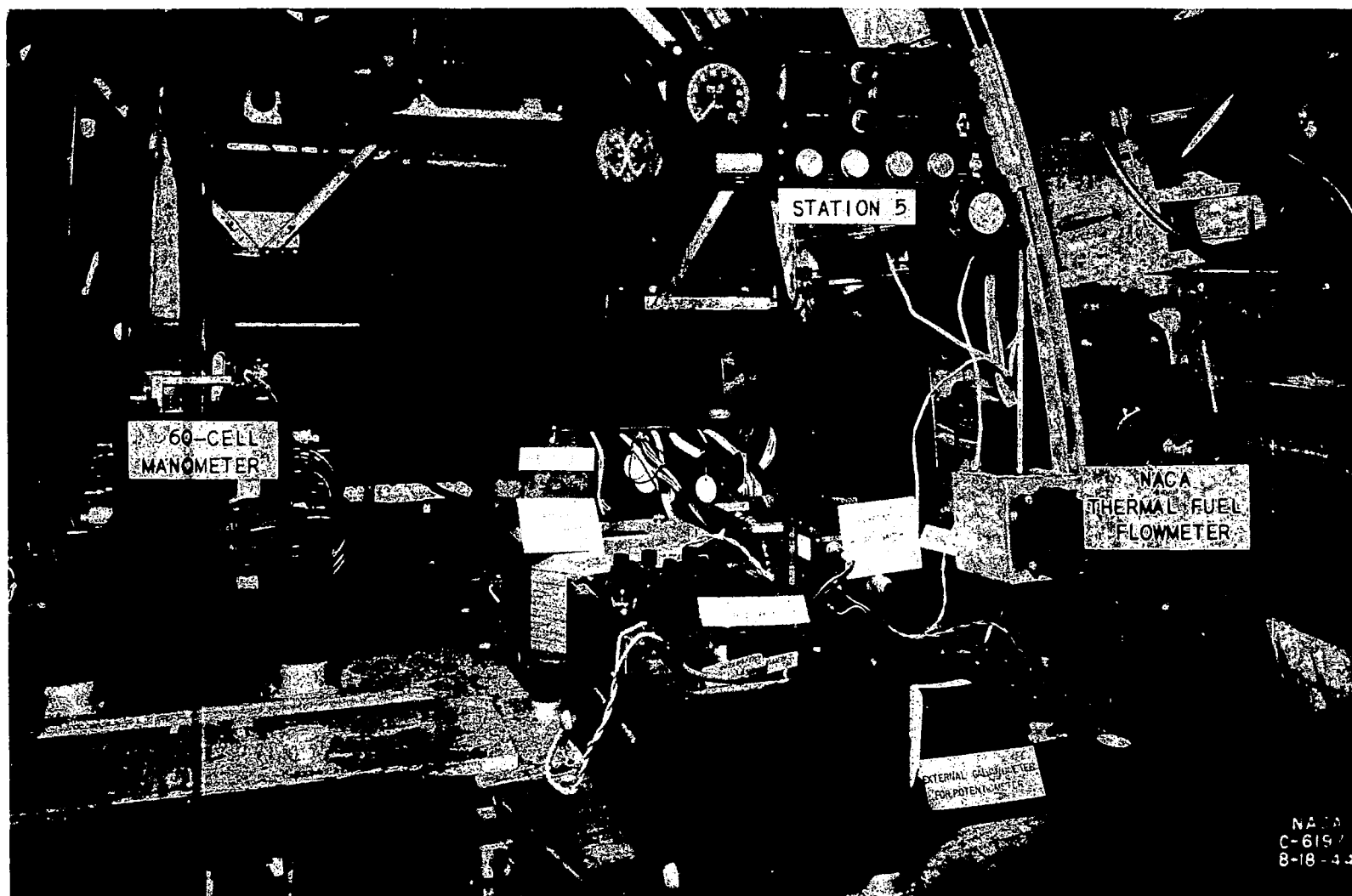


Figure 29. - Station 5. Instruments for recording temperatures, fuel flow, and reference voltage and temperatures.

NACA
C-6197
8-18-44

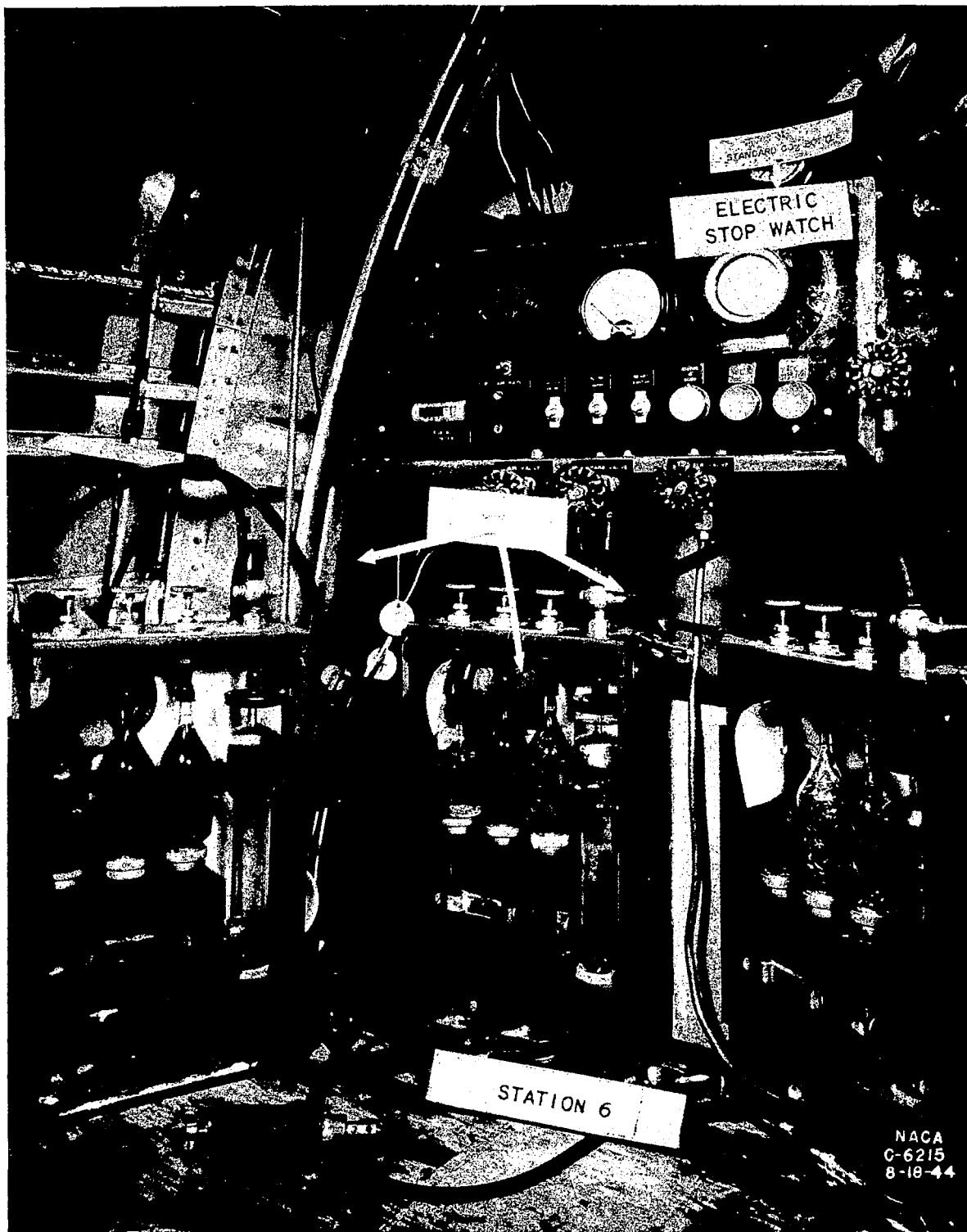


Figure 30. - Station 6. Orsat apparatus for determining fuel-air ratio from exhaust gas.

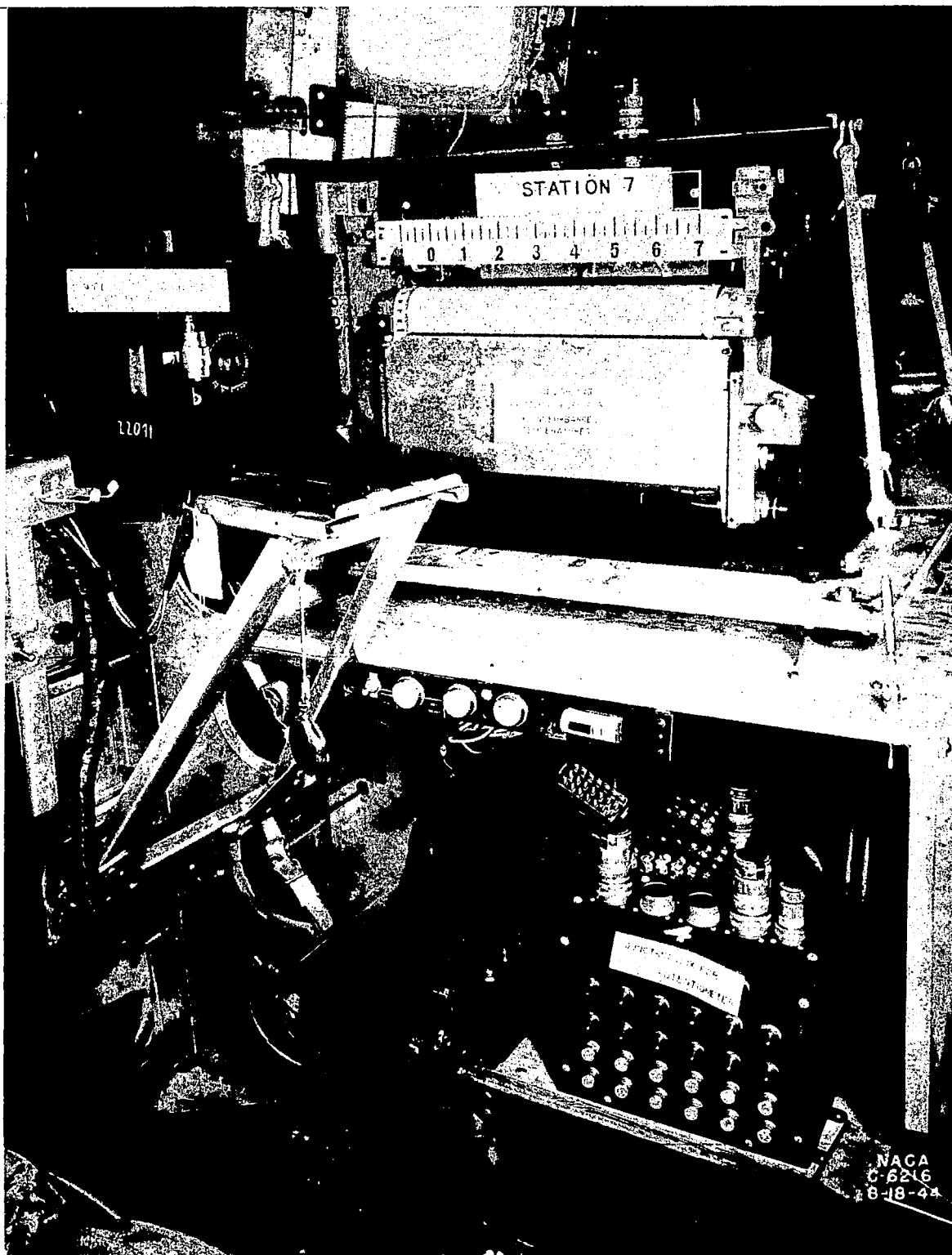


Figure 31. - Station 7. Potentiometer for recording temperatures and camera for filming 100-tube manometer.

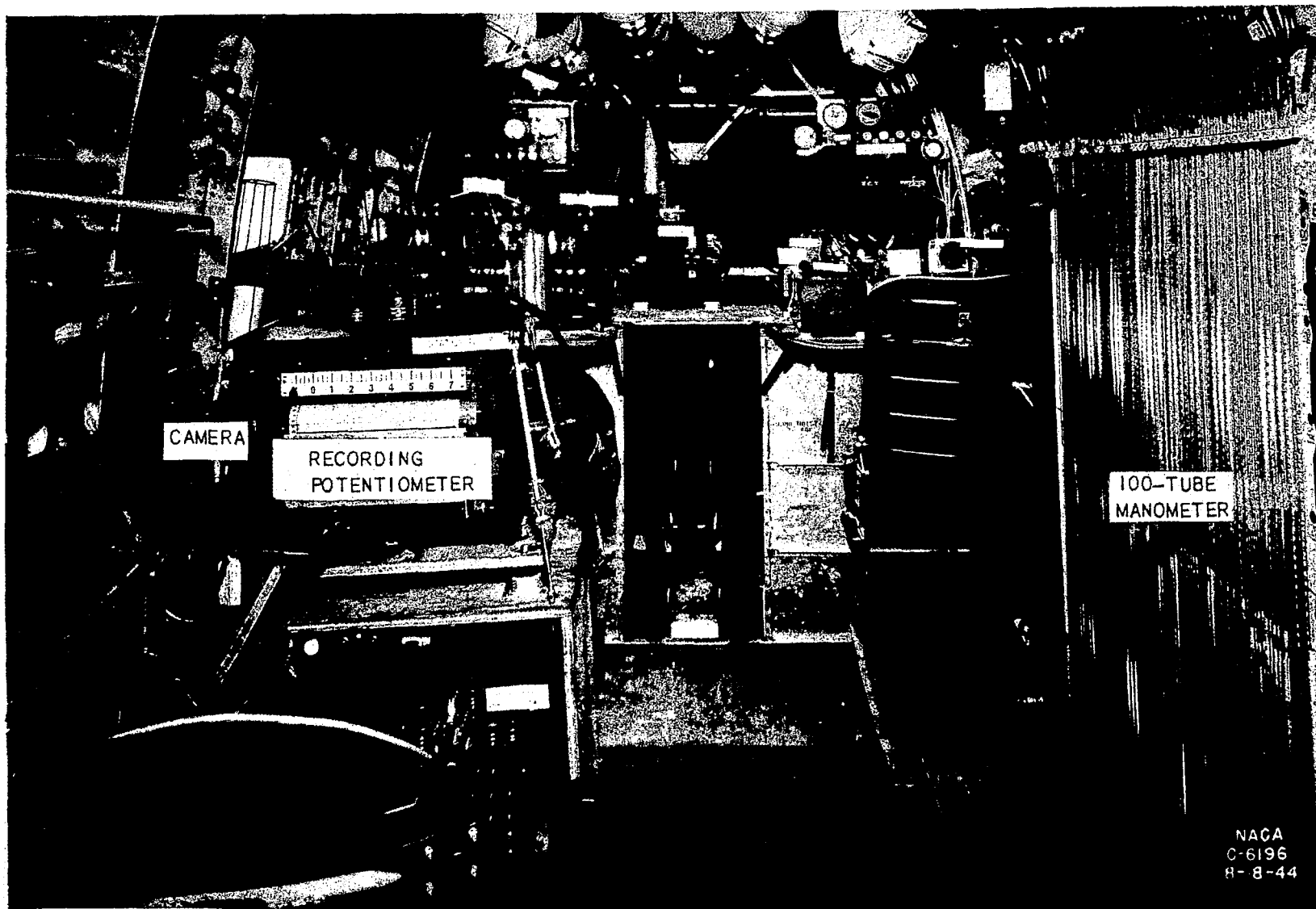


Figure 32. - Rear compartment of four-engine airplane.

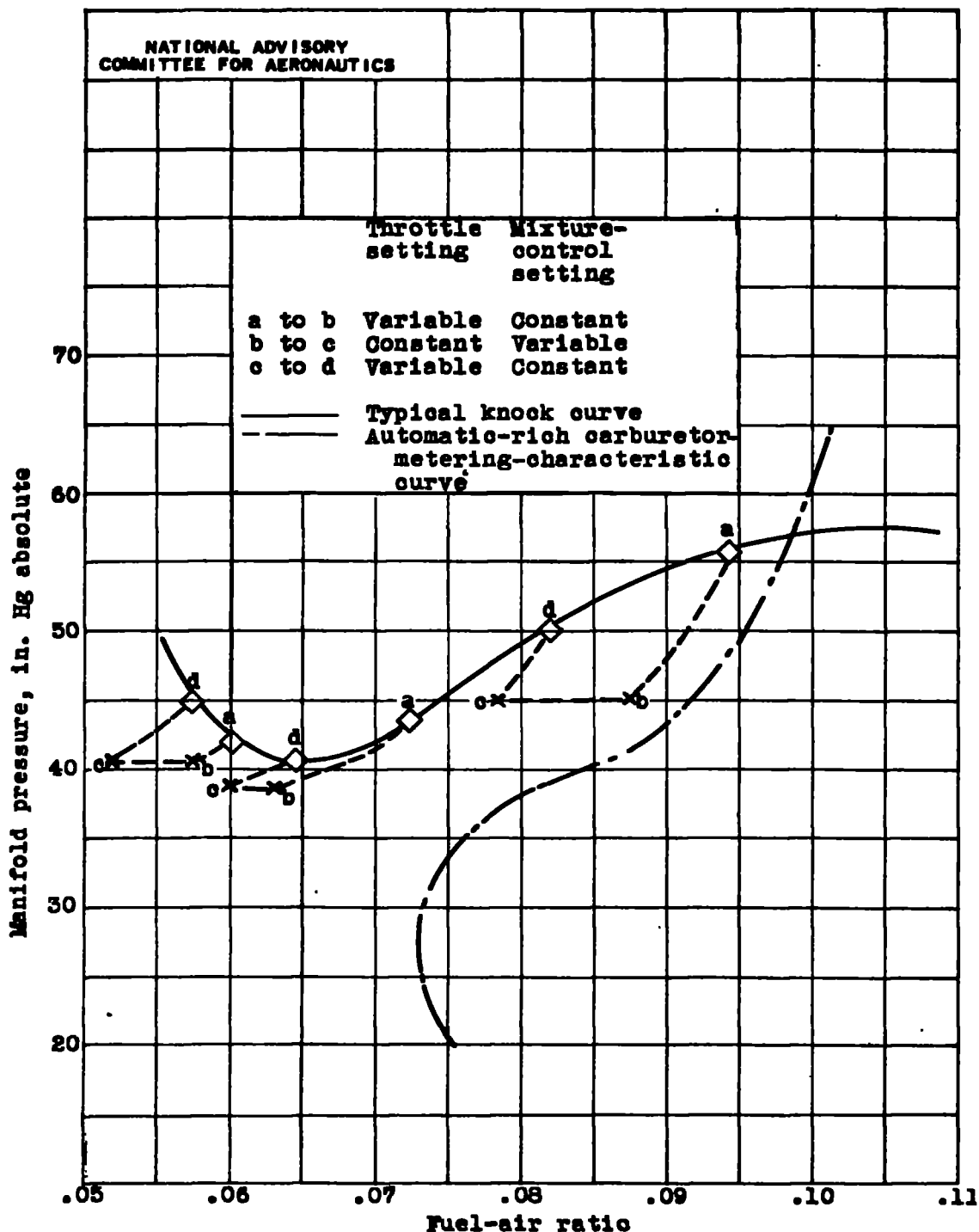


Figure 33. - Procedure used in setting knock points in flight tests.

LANGLEY RESEARCH CENTER



3 1176 01363 8433